

An efficient method of improving essential oil retention and sustained release of chitosan films: Ultrasound-assisted preparation of chitosan composites with surface active chickpea proteins

Pelin Barış Kavur, Ahmet Yemenicioğlu*

Department of Food Engineering, Faculty of Engineering, Izmir Institute of Technology, 35430, Gülbahçe Köyü, Urla, Izmir, Turkey

ARTICLE INFO

Keywords:
Chitosan
Chickpea protein
Composite
Eugenol
Ultrasound
Encapsulation

ABSTRACT

This work aimed at preparing chitosan (CHI) composites with surface active chickpea protein (CP) showing better eugenol (EUG) retention and sustained release capacity than pristine CHI films. For this purpose, ionic complexation of CHI with CP (CHI:CP ratio = 2:1, w/w) in the presence of EUG at pH 5.0 was achieved using mechanical homogenization alone (H_M) or in combination with ultrasonic homogenization (H_M-H_{US}). The H_M-H_{US} treatment provided better solubility of CP (4.4-fold), increased emulsified EUG in film-forming solutions, and denser films than H_M treatment. The composite films obtained using H_M-H_{US} (FLM_{CHI-CP-EUG/H_{M-H_{US}}) retained 1.2–1.4-fold higher EUG after drying, and showed almost 2-fold slower EUG release in air at room temperature than composite films prepared by H_M , and control CHI films prepared by H_M (FLM_{CHI-EUG/H_M}) or H_M-H_{US} (FLM_{CHI-EUG/H_{M-H_{US}}). The FLM_{CHI-CP-EUG/H_{M-H_{US}} films also showed better moisture barrier and mechanical properties than other films. The developed films were proved in a challenging coating application with onions. *Escherichia coli* and *Listeria innocua* counts of inoculated and FLM_{CHI-CP-EUG/H_{M-H_{US}} (average coating thickness = $4.5 \pm 1.3 \mu\text{m}$) coated onions were significantly lower than those of uncoated (2.8 and 3.8 log) and FLM_{CHI/H_{M-H_{US}} (1.4 and 1.3 log) coated onions after 5-days at room temperature. FLM_{CHI-CP-EUG/H_{M-H_{US}} coating also reduced percentage of sprouted onions from 30 to 10% during storage. EUG odor of coated onions could not have been detected by 80% of panelists after 4 weeks. Compositing with CP boosts the performance of essential oil loaded CHI films by enabling use of film matrix as an encapsulant.}}}}}}

1. Introduction

Due to its unique inherent antimicrobial properties chitosan (CHI) is the most promising edible film material employed for active packaging and coating of food (Chen et al., 2023; Verlee, Mincke, & Stevens, 2017; Wang, Qian, & Ding, 2018). The incorporation of CHI with natural antimicrobials has also been attracting a growing interest since this creates an additive or synergistic antimicrobial mechanism that allows effective inhibition of spoilage or pathogenic microorganisms by use of minimum amounts of antimicrobials (Dash, Kumar, & Pareek, 2020; Esmaeili et al., 2020; Upadhyay et al., 2015). The minimization of antimicrobial concentrations in the films is important, especially for essential oils (EOs) that found limited food applications due to their distinctive odor and taste incompatible with the desired sensory properties of most foods (Gutierrez, Barry-Ryan, & Bourke, 2008; Ayala-Zavala, González-Aguilar, & Del-Toro-Sánchez, 2009; Perumal et al., 2022). The

encapsulation is an effective strategy that reduces not only the perception of undesired odor and taste of EOs, but also prevents their loss during film preparation and drying, and allows sustained release of necessary amounts of EO from films on to food surfaces during storage (Yemenicioğlu, 2022). In general, the encapsulation of EOs was applied before they were incorporated into the packaging (Froio et al., 2019; Sharma, Mulrey, Byrne, Jaiswal, & Jaiswal, 2022; Zhang, Jiang, Rhim, Cao, & Jiang, 2022). However, the use of previously encapsulated active components reduces the economic feasibility of edible films and coatings since this needs investment for a separate facility using sophisticated technology and equipment (e.g., homogenizers-dispersers, extruders, or dryers). In contrast, the use of a film matrix as an encapsulant is an alternative practical strategy that allows spontaneous encapsulation of active film components by hydrocolloids or lipids added during homogenization of film-forming solution (Yemenicioğlu, 2022). This strategy is frequently employed for encapsulation of

* Corresponding author.

E-mail address: ahmetyemenicioğlu@iyte.edu.tr (A. Yemenicioğlu).

flavoring agents including EOs incorporated into edible films (Esmaeili et al., 2020; Hambleton, Debeaufort, Bonnotte, & Voilley, 2009; Marcuzzo, Sensidoni, Debeaufort, & Voilley, 2010; Sabphon et al., 2020; Shen et al., 2023; Xue, Gu, Li, & Adhikari, 2019; Zhang, Liang, Li, & Kang, 2020).

Chickpeas have been increasingly used as a source of commercial protein isolates and concentrates to meet the huge demand of the growing plant proteins market. Chickpea protein (CP) is highly popular among regular consumers and vegans as food ingredient due to its light color and neutral taste, free from undesired flavors associated with some legume proteins (e.g., beany flavor of pea proteins). Unlike CHI, which has weak surface activity (Elsabee, Morsi, & Al-Sabagh, 2009; Schulz, Rodríguez, Del Blanco, Pistonesi, & Agulló, 1998), CPs are well-known with their outstanding oil-binding and surface active properties (Aydemir & Yemencioğlu, 2013). Although reports related to the use of CP in edible film matrixes as an encapsulating component of EOs are scarce, these highly functional proteins and their mixtures with other hydrocolloids have been effectively used for encapsulation of hydrophobic substances such as oils (Karaca, Nickerson, & Low, 2013; Moser, Ferreira, & Nicoletti, 2019), essential oil (Atli, Karaca, & Ozelik, 2023) and polyphenol (Ariyaratna & Karunaratne, 2016; Shakoor, Pamunuwa, & Karunaratne, 2023a, b). Therefore, it is thought that blending CHI with highly surface active CP and application of ultrasonic homogenization during film preparation could maximize essential oil emulsification, and enhance retention and sustained release of these volatile active components from composite films. Moreover, the ability of CHI to form polyelectrolyte complexes with anionic proteins (Hein, Wang, Stevens, & Kjems, 2008) could also be exploited to obtain a denser film matrix from CHI-CP complexes and to achieve better sustained release properties for EOs as well as to obtain unique mechanical and barrier properties for the resulting composites.

The primary objective of the current work is to develop novel chitosan (CHI) - chickpea protein (CP) composite films showing better retention and sustained release properties for incorporated eugenol (EUG) than pristine CHI films. Moreover, it is also aimed that the effectiveness of the developed films are shown in an application on a proper model food. The EUG, a generally recognized as safe (GRAS) volatile phenol that forms up to 90% of clove essential oil (Santin et al., 2011; Santos, Chierice, Alexander, Riga, & Matthews, 2009; Zhang et al., 2017), could be an ideal antimicrobial coating component for onions that are frequently linked with outbreaks and recalls due to pathogens such as *Escherichia coli* O157:H7, *Listeria monocytogenes* and *Salmonella* spp. contaminating onions mostly by contact with soil (CDC, 2016; 2020, 2021; FDA, 2022; NBPSDHU, 2009). The EUG is not only an effective antimicrobial for most human pathogenic bacteria (Almeida et al., 2023; Oussalah, Caillet, Saucier, & Lacroix, 2007), but also an effective antimicrobial against plant pathogenic bacteria and fungi (Alkan & Yemencioğlu, 2006; Hu et al., 2019; Morcia, Malnati, & Terzi, 2012; Xie, Huang, Wang, Cao, & Zhang, 2017). The EUG is also responsible for the antimicrobial potency of clove EO that is an effective antimicrobial for *Pectobacterium carotovorum* subsp. *carotovorum* responsible for onion soft rot (Zhang et al., 2023) and *Aspergillus niger* causing black mold in onions (Devi & Rajini, 2021). The clove EO and EUG are also well-known with their antisprouting activity (Finger et al., 2018; Kleinkopf, Oberg, & Olsen, 2003; Santos, Araujo, Lima, Costa, and Finger, 2020). The inhibition of sprouting by EOs and their components is generally attributed to their effect on the synthesis and activity of plant hormones (Clegg, Middleton, Bell, & White, 1980; Gumbo, Magwaza, & Ngobese, 2021; Oosterhaven, Hartmans, & Huizing, 1993; Suttle, Olson, & Lulai, 2016). Thus, the use of GRAS phenolic compound EUG as an antimicrobial and antisprouting agent could prevent great economic losses in onions and reduce commercial use of synthetic antisprouting agents (e.g., maleic hydrazide) that cause growing health concerns. This work is innovative in that it developed a novel CHI-based composite coating material using CP to emulsify and encapsulate EUG in the film matrix, and employed this material as an antimicrobial and

antisprouting coating on onions for the first time in the literature.

2. Materials and methods

2.1. Materials

Chitosan (molecular weight: 50–190 × 10³ Da, deacetylation: 75–85%) and eugenol (E51791) were obtained from Sigma-Aldrich (St. Louis, MO, USA). Glycerol and Tween 80 (hydrophilic/lipophilic balance, HLB = 15.0) were purchased from Merck (Darmstadt, Germany). *Listeria innocua* NRRL-B 33314 (ATCC 1915) and *Escherichia coli* RSHM 4024 (ATCC 25922) were from culture collection of the microbiology laboratory of the Department of Food Engineering at Izmir Institute of Technology. Whole fresh shallots (average weight: 5.0 ± 1.0 g) free from defects and signs of sprouting were purchased from a local market.

2.2. Methods

2.2.1. Preparation of chickpea protein concentrate

Chickpea protein concentrate was obtained using alkaline extraction and following isoelectric precipitation (IEP) method. For this purpose, 50 g of dry Kabuli type chickpeas were rehydrated overnight in 500 mL of deionized water at 4 °C. The mixture was then homogenized in a Waring blender equipped with a stainless steel jar for 2 min at high speed. For protein isolation, the pH of the homogenate was adjusted to 9.5 with 1 M NaOH and stirred using magnetic stirrer for 45 min at ambient temperature. The slurry was first filtered through cheesecloth and then clarified by centrifugation for 15 min at 9600×g and 4 °C (Sigma 6K15 centrifuge, Osterode am Harz, Germany). The supernatant was collected and then its pH was adjusted to 4.5 with 1 M acetic acid to precipitate the extracted proteins. The precipitate was collected by centrifugation and resuspended in distilled water. The isoelectric precipitation at pH 4.5 and centrifugation were repeated, and the collected precipitate was resuspended in distilled water. The protein solution was then lyophilized (Labconco, FreeZone, 6 L, Kansas City, MO, USA) after adjusting its pH to 7.0, and obtained powder was stored at –18 °C. The total protein and carbohydrate contents of the obtained chickpea protein concentrate determined by Kjeldahl and phenol-sulphuric acid methods were 70% and 20% w/w, respectively.

2.2.2. Preparation of film-forming solutions by mechanical homogenization (H_M)

Different film-forming solutions (FFSs) were prepared as follows; the basic CHI FFS (FFS_{CHI}) was prepared by solubilization of CHI at a concentration of 1.5% (w/w) in 0.5% (v/v) acetic acid solution by stirring at 300 rpm for 20 h. The FFS_{CHI} was used for preparation of control CHI films or CHI-CP composite films. The composite FFS (FFS_{CHI-CP}) was prepared by suspending CP at 0.75% (w/w) in FFS_{CHI} (CHI:CP ratio = 2:1, w/w). Then, both FFS_{CHI} and FFS_{CHI-CP} were treated by mechanical homogenization at 12,000 rpm for 3 min using a homogenizer-disperser (Heidolph Instruments, Silent Crusher M, Schwabach, Germany). The FFS_{CHI} and FFS_{CHI-CP} treated only by mechanical homogenization for 3 min were named FFS_{CHI/H_M} and FFS_{CHI-CP/H_M}, respectively. The FFSs were then filtered using a cheesecloth to remove air bubbles and insoluble residues. Then, glycerol at 1.5% (w/w) and Tween 80 at 0.1% (w/w) were added into each FFS as plasticizer and surface active agent by stirring at 300 rpm for 30 min, respectively. After that EUG at a concentration of 0.64% (w/w) was added into each solution with subsequent stirring at 800 rpm for 15 min. To emulsify the added EUG, the dispersions of FFS_{CHI/H_M} and FFS_{CHI-CP/H_M} were further homogenized at 15,000 rpm for 5 min. After addition of EUG, the specified FFSs were abbreviated as FFS_{CHI-EUG/H_M} and FFS_{CHI-CP-EUG/H_M}. The controls, FFS_{CHI/H_M}, FFS_{CHI-CP/H_M}, lacking EUG were also treated with additional mechanical homogenization for 5 min.

2.2.3. Preparation of film-forming solutions by mechanical homogenization and ultrasonic homogenization (H_M-H_{US})

The FFS_{CHI} and FFS_{CHI-CP} were prepared by mechanical homogenization for 3 min as described in 2.2.2. Then, the FFSs were further treated by ultrasonic homogenization at ambient temperature using a processor (Vibra-Cell VC505, Sonics & Materials Inc., Newtown, CT, USA) with an ultrasonic probe of 13 mm in diameter operating at the frequency of 20 kHz. One hundred milliliter portions of the FFS_{CHI} or FFS_{CHI-CP} were treated in 150 mL glass beakers by immersing probe to a depth of almost 3 cm and applying sonication at 75% amplitude for 10 min at 500 W (1st US). The samples treated both by mechanical homogenization and sonication were named FFS_{CHI/H_M-H_{US}} and FFS_{CHI-CP/H_M-H_{US}}, respectively. All FFSs were then filtered using a cheesecloth to remove air bubbles and insoluble residues. Then, glycerol at 1.5% (w/w) and Tween 80 at 0.1% (w/w) were added into each FFS as plasticizer and surface active agent by stirring at 300 rpm for 30 min, respectively. After that EUG at a concentration of 0.64% (w/w) was added into each solution with subsequent stirring at 800 rpm for 15 min. To emulsify the added EUG, the dispersions were first homogenized at 15,000 rpm for 3 min, and then they were further treated by sonication for 2 min (at similar sonication conditions described above) (2nd US). The obtained FFS with EUG were abbreviated FFS_{CHI-EUG/H_M-H_{US}} and FFS_{CHI-CP-EUG/H_M-H_{US}}. The controls lacking EUG were also treated with additional ultrasonication for 2 min and abbreviated as FFS_{CHI/H_M-H_{US}} and FFS_{CHI-CP/H_M-H_{US}}.

2.2.4. Preparation of edible films

The classical solution-casting method was used to obtain self-standing films for characterization studies. For this purpose, 20 g portions of film-forming solution were poured into disposable Petri dishes (8.5 cm in diameter), and the dishes were dried at 45 °C for 20 h. The films peeled-off from the Petri dishes were used in different analyses [Note: the concentrations of CP and EUG used in film-forming solutions were optimized with detailed preliminaries. Effects on film-forming and mechanical properties were evaluated for CP while EUG was evaluated for its effect on film-formation and minimum inhibitory concentrations on *L. innocua* and *E. coli* (see method and results in Supplementary file, Tables S1 and S2). The films obtained from different FFS were abbreviated only by replacing FFS in the abbreviations as FLM (film) (e.g., film from FFS_{CHI-CP-EUG/H_M-H_{US}} was abbreviated FLM_{CHI-CP-EUG/H_M-H_{US}}]. Film thickness was measured using a digital micrometer (Palmer, Comecta, Barcelona, Spain).

2.2.5. Physicochemical properties of film-forming solutions

Soluble protein contents of FFSs were determined by the Bradford assay (Bradford, 1976) using bovine serum albumin (BSA) (Sigma-Aldrich, St. Louis, MO, USA) as protein standard. Results were expressed as g soluble protein per 100 g of each FFS. Experiments of each solution were replicated twice with three repetitions.

Emulsion stabilities of FFSs were determined by monitoring turbidities of EUG containing FFSs using both a spectrophotometer (Shimadzu UV-Vis, Model 2450, Japan) and a turbidimeter (HACH, 2100 AN, USA) by the methods given by Ziani, Fang, and McClements (2012) and Zidan et al. (2007), respectively. The wavelength was set to 600 nm for the spectrophotometric method. Experiments of each solution were replicated twice with two repetitions. For turbidimetric method, 30 mL of freshly prepared samples were filled into the screw-capped cylindrical bottles and the results were given in nephelometric turbidity unit (NTU). The measurements were done at different time intervals during 28 days at room temperature for samples kept in reading bottles.

EUG retention levels of FFSs were determined by assaying their total phenolic content by Folin-Ciocalteu method (Singleton & Rossi, 1965). The retention levels (%) were calculated considering the ratio of the calculated amount of EUG in FFS after 10 days of cold storage at 4 °C to the initial amount of EUG added into FFS. Experiments of each solution were replicated twice with three repetitions.

Particle size distributions of FFSs were monitored using laser diffraction particle size analyzer (Mastersizer 3000, Malvern Instruments, Malvern, UK) fitted with a Hydro EV which is the liquid samples dispersion unit. The results of droplet size expressed as volume-weighted mean particle diameter ($D[4,3]$) were given as μm . Experiments of each solution were replicated twice with three repetitions.

Zeta (ζ -) potential values of FFSs were determined using a zeta potential analyzer (NanoPlus 3, Particulate Systems, Micromeritics, GA, USA) at ambient temperature. Solutions were 10-fold diluted with 0.01 M acetate buffer adjusted to 5.0 pH and directly injected into the capillary cell of the analyzer. Experiments of each solution were replicated twice with three repetitions.

pH was directly measured by immersing probe of a digital pH-meter (inoLab, Terminal, Level 3, WTW GmbH, Weilheim, Germany) into FFSs. Experiments of each solution were replicated twice with two repetitions.

The light transmittances of FFSs were determined by measuring their transmittance (T%) at 600 nm using a spectrophotometer (Shimadzu UV-Vis, Model 2450, Japan). Experiments of each solution were replicated twice with two repetitions.

For the microstructural investigation, 1 mL of film-forming solution (FFS_{CHI-CP-EUG/H_M} or FFS_{CHI-CP-EUG/H_M-H_{US}}) was dyed using 5 μL fluorescent stain Nile Red (1 mg/mL ethanol) in the dark. A drop of stained sample was placed on a glass slide, covered with a coverslip and visualized with a fluorescence microscope (Zeiss Observer Z1, Germany). Digital images were taken with a final magnification of 50x (10x ocular and 5x objective lens) and 630x (10x ocular and 63x objective lens, immersion oil).

2.2.6. Physicochemical properties of films

Film solubility (S) and swelling (SW) tests were performed according to the gravimetric method described by Ferreira et al. (2016) with slight modifications. Films (15 mm \times 7.5 mm) were dried in a vacuum oven (Barnstead Lab-Line, Model 3608-6CE, USA) at 70 °C for 24 h and weighed (W_1). Then, dried films were placed in Petri dishes with 10 mL of distilled water, and shaken at 80 rpm and 25 °C for 24 h. After that the films collected carefully were weighed (W_2), dried again overnight at 70 °C and weighed again (W_3). Results were expressed as percent using equations (1) and (2). Experiments of each film were replicated twice with five repetitions.

$$S (\%) = [(W_1 - W_3) / W_1] \times 100 \quad (1)$$

$$SW (\%) = [(W_2 - W_1) / W_1] \times 100 \quad (2)$$

Optical properties of films (10 mm \times 30 mm) were determined by measuring transmittances at 280 nm (T_{280}) and 600 nm (T_{600}) using a spectrophotometer (Shimadzu UV-Vis, Model 2450, Japan). Opacity (O) was calculated from equation (3) given by Han and Floros (1997). Experiments of each film were replicated twice with three repetitions.

$$\text{Opacity (O)} = \text{Abs}_{600} / \text{mean film thickness (mm)} \quad (3)$$

Color of films was measured using a digital colorimeter (chroma meter type, Konica Minolta, CR-400, Tokyo, Japan associated with illuminant D65, standard observer 2° and illumination area of 8 mm diameter) standardized with a white standard plate ($Y = 93.80$, $X = 0.3159$, $y = 0.3322$). The measured CIE; L^* , a^* and b^* values were used for calculation of color difference (ΔE^*) relative to a white color plate using equation (4) given by Gennadios, Weller, Hanna, and Froning (1996). Experiments of each film were replicated twice with five repetitions.

$$\Delta E^* = \left[(L^*_{\text{standard}} - L^*_{\text{sample}})^2 + (a^*_{\text{standard}} - a^*_{\text{sample}})^2 + (b^*_{\text{standard}} - b^*_{\text{sample}})^2 \right]^{1/2} \quad (4)$$

where values in the parenthesis are differences between those of sample and the white standard plate ($L^* = 97.54$, $a^* = -5.02$, $b^* = 7.05$) used as

background.

2.2.7. Water vapor permeability of films

The water vapor permeability (WVP) of films (diameter: 6 cm) was determined using Payne cups (Elcometer 5100, 10 cm² orifice area, England) containing 3 g of dried silica beads according to ASTM Standard Method E96-95 (ASTM, 1995) at 50% relative humidity (RH) and 25 °C. The weights of the cups were recorded at 3 h intervals over a 48 h period. The measured WVP (g·mm/m²·day·kPa) of the films was calculated from equation (5). Experiments of each film were replicated twice with two repetitions.

$$WVP = \frac{\Delta W \cdot L}{t \cdot A \cdot \Delta P} \quad (5)$$

where $\Delta W/t$ is the flux calculated as the slope obtained by linear regression of mass gain of the film (g) versus time (s), L is the mean film thickness (mm), A is the area of exposed film (m²), and ΔP is the partial water vapor pressure difference (kPa) across the both sides of the film.

2.2.8. Oxygen permeability of films

The oxygen permeability (OP) of selected solution cast films were determined by the oxygen scavenger method given by Zhang, Zhao, and Shi (2016). 3 g of deoxidizing agent (reduced iron powder:sodium chloride:activated carbon ratio = 0.5:1.5:1.0) were placed into Payne cups (Elcometer 5100, 10 cm² orifice area, England) and the cups were then sealed after placing the films. All cups were put into a desiccator containing BaCl₂ saturated solution (90% RH) for 48 h at 25 °C. The measured OP (g·mm/m²·day) of the films was calculated from equation (6). Experiments were performed with five replications.

$$OP = \frac{(m_t - m_0) \cdot L}{t \cdot A} \quad (6)$$

where m_t and m_0 are, respectively, the final and initial weights of the cups, L is the mean film thickness (mm), t is time (day), A is the area of exposed film (m²).

2.2.9. Mechanical properties of films

Mechanical properties of films were evaluated by measuring their tensile strength (TS), elongation at break (EB), Young's modulus (YM) and toughness (T) using TA.XT plus texture analyzer (Stable Micro Systems Ltd., Godalming, UK) equipped with tensile grips (crosshead speed: 50 mm/min, initial grip distance: 50 mm, cell load: 5 kg) according to ASTM Standard Method D882-02 (ASTM, 2002). For this purpose, films were cut into 8 mm wide and 80 mm length strips. Tensile properties were calculated from stress-strain curve. Experiments of each film were replicated twice with five repetitions.

2.2.10. Morphological properties of films

The surface and cross-section morphologies of films were examined using a scanning electron microscope (SEM) (FEI Quanta 250 FEG, FEI Company, USA). The films investigated for their cross-sectional SEM were fractured in liquid nitrogen. Micrographs were taken at 5000x and 2500x magnification for surface and cross-sections, respectively.

The surface topologies of films were examined using an atomic force microscope (AFM) (Digital Instruments, MMSPM Nanoscope 8, Bruker, USA). Film samples with an area of 2 μm × 2 μm were scanned at a rate of 1 Hz using tapping mode in the air at ambient temperature using Bruker NCHV model probe (with a spring constant 40 N/m at a resonance frequency of 320 kHz, tip radius 8 nm). The captured images (minimum 3 for each sample) were analyzed by Nanoscope Analysis software, version 1.5 (Bruker, USA). Arithmetic mean roughness (R_a) was also measured for quantitative description.

2.2.11. EUG release kinetics of films in air

To determine the release kinetics of EUG in air, discs of films

(diameter: 8.5 cm) were exposed to air at room temperature or refrigerated storage temperature at 10 °C for 3 weeks. Pieces from films (≈14 cm²) were periodically analyzed for their retained EUG. For this purpose, film pieces were homogenized at 18,000 rpm for 3 min in 5 mL pure ethanol. The extract was then centrifuged at 10,000×g for 15 min, and the EUG in the extracts were determined spectrophotometrically as given in 2.2.12. The EUG retention in the films was analyzed by first-order reaction kinetics. The retention curves were formed by plotting log retained EUG contents (%) vs. time (h). First-order rate constants (k) were determined from the slope of the initial linear portion of curves. The half-life (T_{1/2}) of EUG loss (the time needed for 50% loss of retained EUG in films by evaporation at ambient temperature) was calculated from equation (7). Experiments of each film were replicated twice with three repetitions.

$$T_{1/2} \text{ (day)} = \ln(2) / k \quad (7)$$

2.2.12. Soluble EUG contents of films released in different food simulants

The soluble EUG contents of films were determined by release tests performed in aqueous food simulant (simulant A: ethanol at 10%, v/v) and fatty food simulant (simulant D1: ethanol at 50%, v/v) (EU Regulation No 10/2011). Film samples (3 cm × 6 cm) were placed into flasks containing 50 mL of each food simulant kept under stirring at 80 rpm at 4 °C or 25 °C. The EUG in the extracts was determined periodically until reaching of equilibrium using the spectrophotometric Folin-Ciocalteu method (Singleton & Rossi, 1965). The calibration curve was prepared by dissolving EUG (0.0078–0.25 mg/mL; R² = 0.9872) in ethanol. The percentage of soluble EUG released from films (% soluble EUG) was calculated from equation (8) given below:

$$\text{Soluble EUG (\%)} = [\text{EUG}_{\text{max}} / \text{EUG}_{\text{incorporated}}] \times 100 \quad (8)$$

where EUG_{max} is maximum amount of EUG released from films at the equilibrium (mg/cm²) and EUG_{incorporated} is amount of EUG incorporated into films (mg/cm²). Experiments of each film were replicated twice with three repetitions.

2.2.13. Application of developed films for active coating of shallot onions

Five bulbs were coated each time by dipping into different FFS (≈50 g) for 3 min. The bulbs were drained and placed into sterile Petri dishes without lids. The dish content was dried overnight in a biosafety cabinet at room temperature. All samples were prepared in duplicate. The bulbs were stored at ambient conditions for 28 days and different analyses were carried out periodically.

2.2.13.1. Determination of coating thickness at the onion surface. The thickness of active coating on bulb skin outer surface was determined from cross-sectional images using SEM (FEI Quanta 250 FEG, FEI Company, USA). The skins of bulbs were separated carefully and coated with gold palladium for 1 min in a sputter coater (SPI-Module Sputter Coater Unit, SPI Supplies/Structure Probe Inc., USA) before imaging. Micrographs were taken at 1000x and 2500x magnification for the surface and cross-section of onion skins, respectively.

2.2.13.2. Physicochemical changes in coated onions during storage. Total soluble solid (TSS) content of bulbs was determined using a digital refractometer (Atago 3830, PAL-3, Tokyo, Japan) according to Roldán-Marín, Sánchez-Moreno, Lloría, de Ancos, and Cano (2009). Measurements were replicated twice with five repetitions.

pH of bulbs was determined using a digital pH-meter (inoLab, Terminal, Level 3, WTW GmbH, Weilheim, Germany) according to Roldán-Marín et al. (2009). Measurements were replicated twice with five repetitions.

Titrate acidity of bulbs was determined using the colorimetric titration method in accordance with AOAC Official Method 942.15

(AOAC, 2000). Results were expressed as g malic acid/100 g fresh weight (g MA/100 g f.w.). Measurements were replicated twice with five repetitions.

Firmness changes of onion bulbs was measured by a penetration test performed on both at root-end and equatorial regions of onions using a TA.XT plus Texture Analyzer (Stable Micro Systems Ltd., Godalming, England) equipped with a needle probe attachment (crosshead speed: 0.5 mm/s, cell load: 5 kg). Test conditions used by Maw, Hung, Tollner, Smittle, and Mullinix (1996) were applied with slight modifications. A whole bulb was positioned in the center of the platform and the probe penetrated into the polar region of the bulb to 50% from the surface. Then, bulbs were halved vertically, each half was positioned in the center of the platform and the probe penetrated into the equatorial section of the bulb to 75% from the surface. Penetration force (N) that is the maximum force required to insert the needle into bulb to a depth that causes irreversible crushing was determined. Measurements were replicated twice in each of the five bulbs with four repetitions.

2.2.13.3. Determination of antisprouting activity of coatings on coated bulbs. The incidence of external sprouting of coated and uncoated bulbs stored at room temperature was examined visually and recorded daily. According to Miedema (1994), a bulb was considered sprouted when the sprout leaves have emerged from the neck. The number of sprouted bulbs was recorded for each group. Moreover, according to the method applied by Temkin-Gorodeiski, Kahan, and Padova (1972), examined bulbs were halved (vertically from top to bottom), and the strength of green coloration in the stalk sprouting from the center of onion bulb was graded visually using a color scale between 1 and 4 (1: white, 2: yellow, 3: yellowish green and 4: green) (see the scale at Supplementary file, Fig. S1). Internal parts of onions were also photographed to record the sprouting status.

2.2.13.4. Antimicrobial activity of film-forming solutions and dried coatings on onions. The onion bulbs were surface-sterilized with 1% (v/v) sodium hypochlorite solution for 15 min and rinsed with sterile distilled water before used in antimicrobial tests. Ten bulbs from each group were disinfected and dried in a ventilated cabinet. Meanwhile, the inoculums were prepared from 150 μ L of stock cultures of *L. innocua* or *E. coli* by transferring into 135 mL 1% (w/v) peptone water (Merck, Darmstadt, Germany) and then incubating at 37 °C for 24 h. The initial number of inocula was 10⁸ cfu/mL. Bulbs immersed into one of the cultures were drained in sterile Petri dishes and dried overnight in a biosafety cabinet. The dried inoculated bulbs were then coated with different FFS as described in section 2.2.13.

The effect of film-forming solutions on microbial load of inoculated onions was determined on the 0th day when coated onions were still wet. For this purpose, the inoculated and dip-coated bulbs were isolated with 10-fold of 1% peptone water by vigorous stirring in an Erlenmeyer flask at 320 rpm for 30 min.

The effect of coatings on microbial load of onions was determined on 1st and 5th days when they were fully dried at 25 °C. The dried coating prevents the isolation of inoculated bulbs by vigorous stirring. Therefore, for isolation of inoculated bacteria in dried coated bulbs, the most outer peel layers of bulbs were carefully peeled with a sterile knife, and a 0.5 g peel sample was homogenized in 10 mL of sterile 1% peptone water at 6000 rpm for 5 min using a high speed miniature dispenser (Ultra Turrax tube dispenser, IKA Werke GmbH & Co. KG, Staufen, Germany). The serial decimal dilutions prepared from 0th-day isolate by vigorous stirring, and 1st- and 5th-day isolates prepared by miniature dispenser were spread-plated onto Oxford Listeria Selective Agar (Merck, Darmstadt, Germany) enriched with Oxford Listeria Selective Supplement (Merck, Darmstadt, Germany) and Violet Red Bile Agar (Merck, Darmstadt, Germany) for enumeration of *L. innocua* and *E. coli*, respectively. The plates were incubated at 37 °C for 24 h and the colonies were counted. Microbiological counts were expressed as log cfu/g

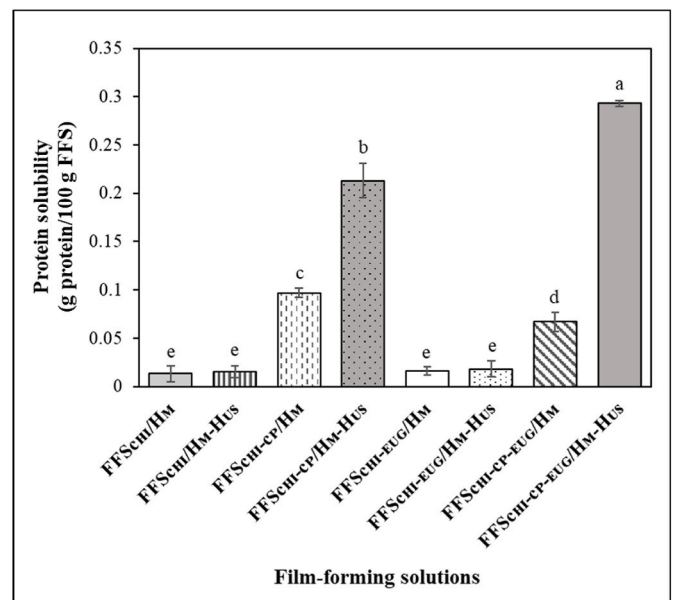


Fig. 1. Effect of ultrasonication (US) and compositing with chickpea proteins (CP) on soluble protein content of different film-forming solutions (H_M: mechanical homogenization; H_M-H_{US}: mechanical homogenization and a following ultrasonic homogenization).

bulb. Experiments of each bulb were replicated twice with three repetitions.

2.2.13.5. Detection of end-point for EUG odor in stored coated onions by a sensory test. End-point odor testing was performed only for onion bulbs coated with FFS_{CHI-CP-EUG}/H_M-H_{US} in the sensory room at Department of Food Engineering in Izmir Institute of Technology by trained panellists. Ten adults aged between 25 and 35 years took part in this evaluation. Uncoated bulbs free from EUG were used as control. After 0, 1, 7, 14, 21, 28 days of ambient storage, bulbs were coded with random three-digit numbers and served to the panellists on trays. The room air was refreshed between each assessment. In sensory evaluation, the panellists were asked if they detect EUG odor in FFS_{CHI-CP-EUG}/H_M-H_{US} coated and uncoated onions based on two response categories “yes” or “no”.

2.2.14. Statistical analysis

One-way analysis of variance (ANOVA) was used to process the data of the characterization of film and FFS samples while two-way ANOVA was performed to evaluate the storage period analysis of active films and coated bulb samples using IBM SPSS Statistics for Windows, version 23.0 (IBM Corp., USA). Statistical differences among means were compared with Duncan’s multiple range test at a significance level of $P < 0.05$.

3. Results and discussion

3.1. Effect of US and CP compositing on physicochemical properties of film-forming solutions

3.1.1. Solubility of CP in film-forming solutions

The primary objective of the US treatment applied before addition of EUG (1st US) was to improve CP solubility essential for its surface active properties. On the other hand, the US applied after addition of EUG (2nd US) aimed mainly emulsification of this EO. The data presented in Fig. 1 clearly showed that the protein solubility of FFS was significantly improved by the US ($P < 0.05$). In fact, the FFS_{CHI-CP}/H_M-H_{US} and FFS_{CHI-CP-EUG}/H_M-H_{US} showed almost 2.2- and 4.4-fold higher soluble protein content than FFS_{CHI-CP}/H_M and FFS_{CHI-CP-EUG}/H_M, respectively. It is interesting to report that H_M alone resulted with significantly higher

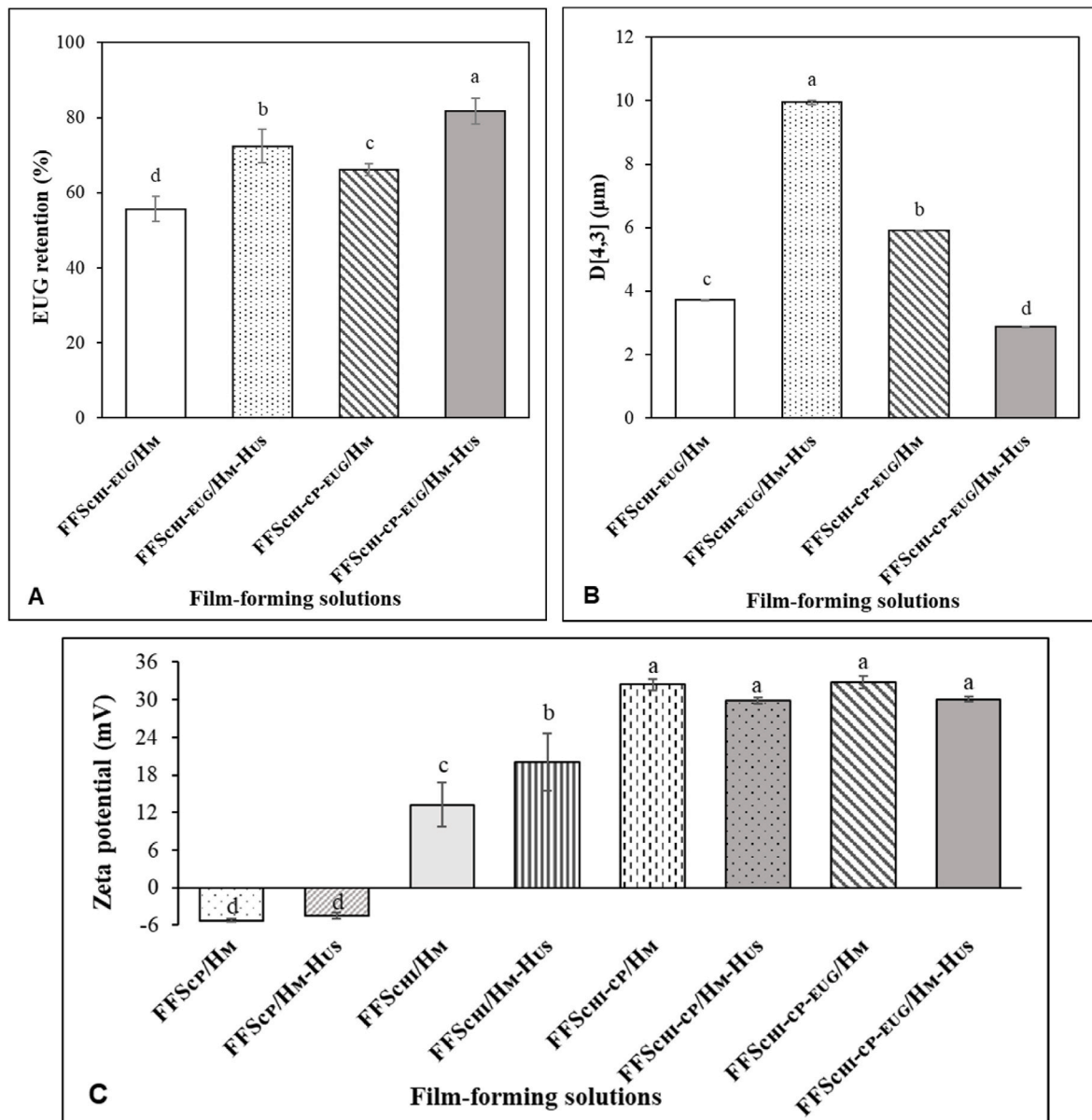


Fig. 2. Effect of US and compositing with CP on EUG retention (A), particle size (B) and ζ -potential (C) values of different film-forming solutions.

(1.4-fold) CP solubility in FFS_{CHI-CP}/H_M than in FFS_{CHI-CP-EUG}/H_M. It seems that H_M in the presence of EUG increased protein aggregation, thus, this caused a reduction in CP solubility. In contrast, the US application after H_M (H_M-H_{US}) caused significantly higher (almost 1.4-fold) CP solubility in FFS_{CHI-CP-EUG}/H_M-H_{US} than in FFS_{CHI-CP}/H_M-H_{US}. This finding suggested that the CP aggregated in the presence of EUG after H_M resolubilized very effectively following the application of US.

3.1.2. EUG retention in film-forming solutions

The results of % EUG retention in FFS after 10 days of cold storage clearly showed the beneficial effect of applying US in the presence of CP to increase amount of emulsified and retained EO in FFS (Fig. 2A). FFS_{CHI-CP-EUG}/H_M-H_{US} showed the highest EUG retention (82%) followed by FFS_{CHI-EUG}/H_M-H_{US} (72%), FFS_{CHI-CP-EUG}/H_M (66%), and FFS_{CHI-EUG}/H_M (56%). The beneficial effect of US on EUG retention was clear as H_M-H_{US} gave greater EUG contents than H_M for FFSs having similar composition. The significantly greater EUG retention in FFS_{CHI-CP-EUG}/H_M-H_{US} than that in FFS_{CHI-EUG}/H_M-H_{US} also clearly showed that CP contributed to an increasing amount of EUG retained in FFS. Moreover, the distribution of emulsified EUG droplets in FFS_{CHI-CP-EUG}/H_M

and FFS_{CHI-CP-EUG}/H_M-H_{US} was also observed using fluorescence microscopy by staining EUG with lipophilic dye Nile Red. The obtained micrographs showed more homogenous distribution of EUG droplets in FFS_{CHI-CP-EUG}/H_M-H_{US} than those in FFS_{CHI-CP-EUG}/H_M (see Supplementary file Fig. S2). These results proved that FFS_{CHI-CP-EUG}/H_M-H_{US} was the best procedure to incorporate EUG into chitosan-based films.

3.1.3. Particle size of film-forming solutions

The D[4,3] particle sizes of different EUG containing FFSs are seen in Fig. 2B. The significantly greater particle size of FFS_{CHI-CP-EUG}/H_M (5.91 μ m) than that of FFS_{CHI-EUG}/H_M (3.71 μ m) suggested that the incorporation of CP by H_M caused an increase in particle size. It appears that the limited solubilization of CP by H_M leads to some protein aggregations causing an increase in the particle size. In contrast, the smallest particle size obtained by FFS_{CHI-CP-EUG}/H_M-H_{US} (2.87 μ m) suggested the beneficial role of US in the solubilization of CP and dispersion of emulsified EUG droplets. This finding is expected as increased solubility of CP by US should have enhanced the emulsification of EUG. On the other hand, it is interesting to report that the largest particle size was obtained for FFS_{CHI-EUG}/H_M-H_{US}. Thus, it appears that the excessive EUG in FFS_{CHI-}

Table 1
Solubility, swelling capacity and water vapor permeability of different films^{a,b}.

Samples	S (%)	SW (%)	WVP (g·mm/m ² ·day·kPa)
FLM _{CHI/H_M}	25.9 ± 2.65 ^d	50.0 ± 8.11 ^{bc}	20.9 ± 1.2 ^a
FLM _{CHI/H_M-H_{US}}	27.6 ± 3.33 ^d	39.7 ± 5.55 ^{cd}	20.3 ± 1.6 ^{ab}
FLM _{CHI-CP/H_M}	30.9 ± 3.10 ^c	35.9 ± 11.39 ^d	19.2 ± 1.4 ^{abc}
FLM _{CHI-CP/H_M-H_{US}}	28.3 ± 3.27 ^{cd}	36.9 ± 5.60 ^d	18.1 ± 1.8 ^{bc}
FLM _{CHI-EUG/H_M}	36.2 ± 2.98 ^b	29.2 ± 9.49 ^d	21.8 ± 1.1 ^a
FLM _{CHI-EUG/H_M-H_{US}}	38.7 ± 2.19 ^{ab}	31.1 ± 5.50 ^d	20.1 ± 2.7 ^{ab}
FLM _{CHI-CP-EUG/H_M}	38.6 ± 4.31 ^{ab}	59.6 ± 13.30 ^{ab}	21.5 ± 1.9 ^a
FLM _{CHI-CP-EUG/H_M-H_{US}}	40.8 ± 2.66 ^a	67.1 ± 11.57 ^a	16.8 ± 1.0 ^c

^a Different lower superscripts in the same column indicate significant difference ($P < 0.05$).

^b Values are presented as mean value ± SD ($n = 10$ for S and SW, and $n = 4$ for WVP).

EUG/H_M-H_{US} has not been emulsified as effectively as that in FFS_{CHI-CP-EUG/H_M-H_{US}}. These findings indicated that CP played an important role in enhancing the stability of classical monolayer emulsion formed by Tween 80 employed in film making.

3.1.4. ζ -potential of film-forming solutions

In the current study, the pH of the FFSs changed between 5.1 and 5.2 (see Supplementary file Table S3), a very narrow range that is over the isoelectric point (pI) of CP (pI ~ 4.1). As expected, the FFS_{CHI/H_M} and FFS_{CHI/H_M-H_{US}} gave a positive ζ -potential due to the amino groups of CHI (Fig. 2C). The significantly higher ζ -potential of FFS_{CHI/H_M-H_{US}} than FFS_{CHI/H_M} suggested improved CHI solubility and/or exposed charges of amino groups due to the linearization of this macromolecule by the application of US. Although it is not a FFS, the ζ -potential of CP prepared at the same concentration as in FFS and treated by H_M or H_M-H_{US} as described in sections 2.2.2 and 2.2.3 was also investigated to understand the effect of these treatments on protein surface charges. At a pH (~5.1) above its pI, the CP treated by H_M or H_M-H_{US} gave quite similar negative ζ -potentials ($P > 0.05$). In contrast, the FFSs with both CP and CHI (FFS_{CHI-CP/H_M}, FFS_{CHI-CP-EUG/H_M}, FFS_{CHI-CP/H_M-H_{US}}, FFS_{CHI-CP-EUG/H_M-H_{US}}) showed similar ($P > 0.05$) positive ζ -potential

values ranging between +30 mV and +33 mV. The significantly higher positive ζ -potential of FFSs obtained from a mixture of CP and CHI than FFS containing only CHI was an evidence that suggested the complexation of CHI with CP. It appears that the complexation occurs via charge-charge interaction between negatively charged groups of CP (basic amino acid side chains) and positively charged amino groups of CHI. As a result, the negative charges of CP were masked and the resulting CP-CHI complex bore mainly positive charges of both macromolecules. This finding indicated that the greater EUG retention in FFS_{CHI-CP-EUG/H_M-H_{US}} than FFS_{CHI-EUG/H_M-H_{US}} could be due to increased positive charge-charge repulsion among emulsified EUG droplets surrounded by positively charged CHI-CP complex.

3.1.5. Transparency/turbidity of film-forming solutions

The control FFSs with only soluble CHI were transparent (see T% values for FFS_{CHI/H_M} = 89.83 ± 3.73% and FFS_{CHI/H_M-H_{US}} = 86.66 ± 0.24% in Supplementary file Table S3), but solubilization of CP formed highly turbid FFSs due to blocking of light by the dispersed protein. A considerably lower transparency was observed for FFS treated by H_M-H_{US} than H_M (T% values for FFS_{CHI-CP/H_M} = 6.24 ± 0.25% and FFS_{CHI-CP/H_M-H_{US}} = 0.30 ± 0.006%) as US treatment increased amount of protein solubilized considerably (see also photos in Supplementary file Figs. S3A and B). The addition of EUG formed opaque (milky) FFSs as a result of emulsion formation (Figs. S3C and D), thus, this prevented passing of light from FFS almost completely (T% values of all EUG containing FFS were ≤0.03%). The turbid and opaque nature of FFS originating mainly from solubilized CP and emulsified EUG were highly stable and showed no considerable change when monitored by different methods for 28 days. However, it should be reported that the FFSs treated by H_M-H_{US} were slightly more turbid than those treated by H_M (see Abs_{600nm} and NTU measurements in Figs. S4A and B by spectrophotometer and turbidimeter, respectively).

3.2. Effect of US and CP compositing on solubility and swelling capacity of edible films

The effect of US and CP on the solubility and swelling capacity of different films are presented in Table 1. FLM_{CHI/H_M} and FLM_{CHI/H_M-H_{US}} films showed the lowest water solubility values that were not significantly different ($P > 0.05$). The addition of EUG increased the solubility of CHI films significantly. Therefore, FLM_{CHI-EUG/H_M} and FLM_{CHI-EUG/H_M-H_{US}}

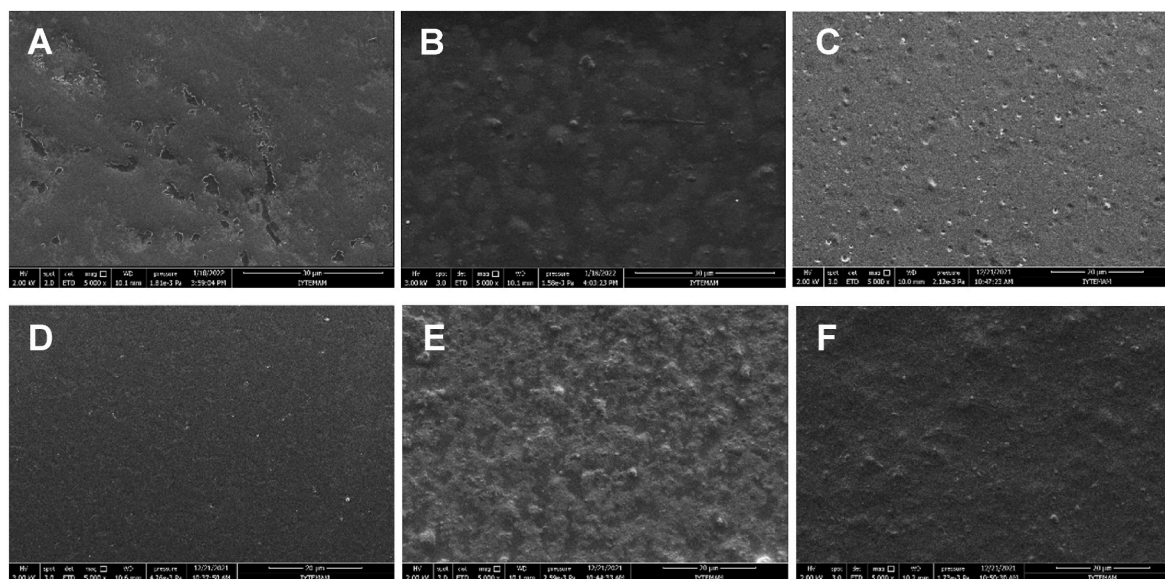


Fig. 3. SEM surface images of different pristine CHI and CHI-CP composite films (magnification = 5000x, A: FLM_{CHI/H_M}, B: FLM_{CHI-CP/H_M}, C: FLM_{CHI-CP-EUG/H_M}, D: FLM_{CHI/H_M-H_{US}}, E: FLM_{CHI-CP/H_M-H_{US}}, F: FLM_{CHI-CP-EUG/H_M-H_{US}}).

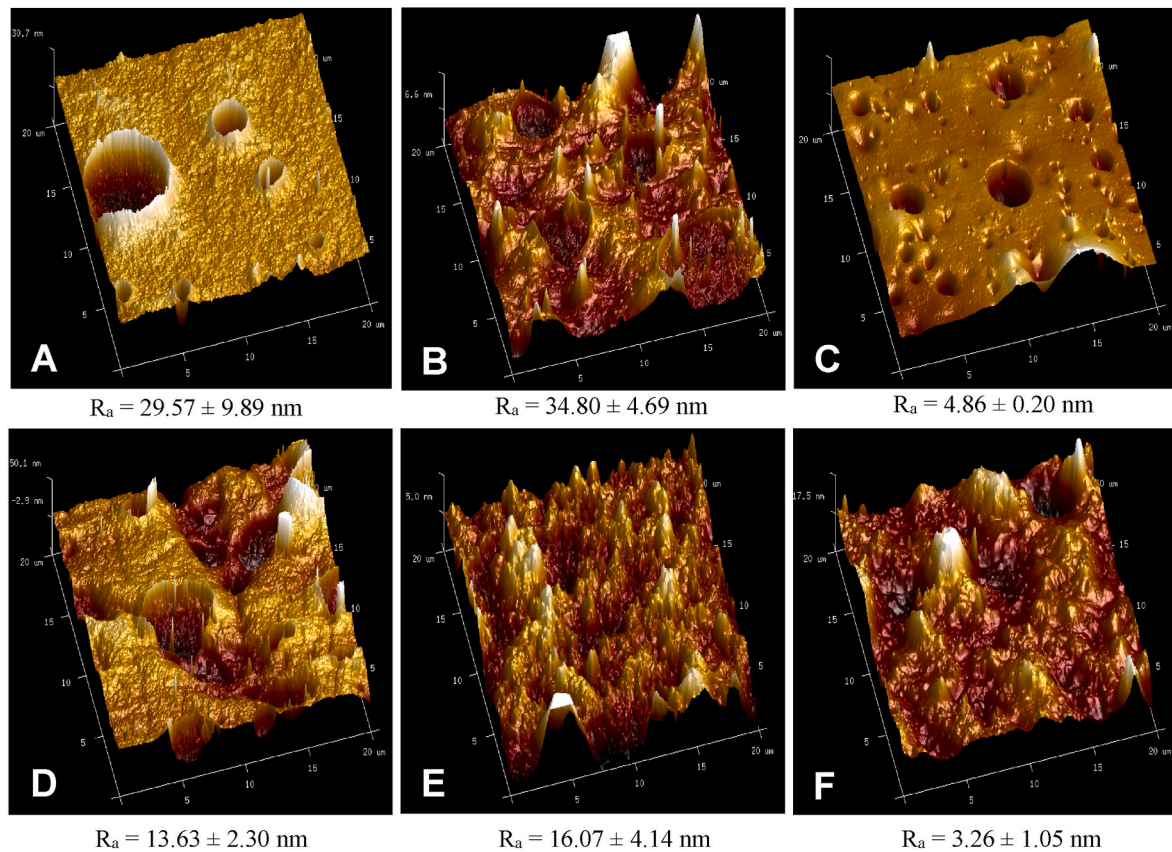


Fig. 4. AFM images of different pristine CHI and CHI-CP composite films (A: FLM_{CHI}/H_M , B: FLM_{CHI-CP}/H_M , C: $FLM_{CHI-CP-EUG}/H_M$, D: FLM_{CHI}/H_M-H_{US} , E: FLM_{CHI-CP}/H_M-H_{US} , F: $FLM_{CHI-CP-EUG}/H_M-H_{US}$).

H_M-H_{US} showed almost 1.4-fold greater solubility than FLM_{CHI}/H_M and FLM_{CHI}/H_M-H_{US} films. The use of CP in film making did not cause a marginal change in solubility of obtained composite films. In fact, the FLM_{CHI-CP}/H_M films showed only slightly higher (1.2-fold) solubility than FLM_{CHI}/H_M films while FLM_{CHI-CP}/H_M-H_{US} and FLM_{CHI}/H_M-H_{US} films showed similar solubility ($P > 0.05$). In contrast, the addition of EUG caused significant increases in solubility of composite films ($P < 0.05$). Thus, these results proved that the incorporated EUG increased the solubility of both CHI and CHI-CP composite films. The interaction of phenolic compounds with hydrocolloids occurs by hydrophobic interactions that form between aromatic rings of phenolic compounds and hydrophobic groups of hydrocolloids (e.g., hydrophobic side chains of amino acid residues in CP, and hydrophobic acetyl groups of chitosan) (Yemencioğlu, 2022). Therefore, it seems that the EUG interacted with hydrocolloids masked the hydrophobic groups of CHI and/or CP and increased their hydrophilicity by its hydroxyl group.

The application of H_M or H_M-H_{US} did not cause a significant effect on the degree of swelling of films having a similar composition ($P > 0.05$). However, the presence of EUG or CP alone in CHI matrix and application of H_M-H_{US} gave a more swelling-resistant rigid film networking than that of pristine CHI film obtained by H_M . It appears that the better solubilization of film components by US caused more interactions created within the film matrix, thus, this resulted in a more limited swelling during the incubation of films in distilled water. In contrast, the presence of both CP and EUG in FFSs gave edible films showing the highest degree of swelling. This result proved that the interaction of EUG with CP within the film matrix enhanced the hydrophilic interactions and this loosened the film matrix during swelling.

3.3. Effect of US and CP compositing on morphological properties of films

3.3.1. SEM images of films

SEM images of surfaces of pristine CHI and CHI-CP composite films are illustrated in Fig. 3. The surface photos of FLM_{CHI}/H_M film showed that the CHI films prepared by H_M had some superficial non-uniform formations that appear as light colored spots at film surface (Fig. 3A). It seems that these are formed by local changes in CHI solubility, possibly by transformation of CHI from amorphous to crystalline form at film surface. Such changes could take place locally around pores during final stages of drying as film-forming solution get concentrated by evaporation. The addition of CP into films caused clearly observed protein aggregates within resulting FLM_{CHI-CP}/H_M composite films (Fig. 3B). The further incorporation of EUG caused disappearance of protein aggregates in $FLM_{CHI-CP-EUG}/H_M$ films. However, unemulsified (free) EUG caused formation of extensive tiny pores and craters at the surface of these composite films prepared by H_M (Fig. 3C). It is evident that the H_M alone is not sufficient for effective emulsification of all EUG, thus, free tiny EO droplets accumulated at the surface of cast FFS, and evaporated during drying left extensive pores and craters at the $FLM_{CHI-CP-EUG}/H_M$ film surface. Similar porous morphologies were observed also by Nisar et al. (2018) at the surface of pectin films due to the phase separation of incorporated clove bud essential oil. In contrast, the application of US gave highly homogenous FLM_{CHI}/H_M-H_{US} films (Fig. 3D). It appears that the application of US reduced the film porosity by emulsification of excessive free EUG and prevented the formation of unemulsified EUG droplets that tend to coalesce at the upper surface of films during film-drying. The addition of CP also caused formation of some protein aggregates in FLM_{CHI-CP}/H_M-H_{US} , but these aggregates were smaller and they distributed much more homogeneously than those in FLM_{CHI-CP}/H_M (Fig. 3E). This finding was expected as effective

solubilization of CP in film-forming solutions by US was demonstrated in the current study (see Fig. 1). The addition of EUG into CHI-CP films by use of US gave more homogenous films (FLM_{CHI-CP-EUG/H_M-H_{US}}) by significant reduction of protein aggregates at the film surface (Fig. 3F). Moreover, FLM_{CHI-CP-EUG/H_M-H_{US}} films did not contain pores and craters at the surface as FLM_{CHI-CP-EUG/H_M} films. This finding proved that the US effectively dispersed CP, emulsified the EUG, and prevented formation of unemulsified free EO droplets that coalesce at the film surface to leave pores and craters following evaporation. The investigation of film cross-sections proved that all films with the exception of FLM_{CHI-CP-EUG/H_M} showed dense film morphologies (see Supplementary file, Figs. S5A–F). The pores observed close to the surface of FLM_{CHI-CP-EUG/H_M} film cross-sections supported our surface observations that part of the EUG cannot be emulsified sufficiently with H_M (Fig. S5C).

3.3.2. AFM images of films

The topographic images of film surfaces obtained by AFM are given in Fig. 4. The FLM_{CHI/H_M} films are characterized by their rough flat surface containing various sizes of circular crater-like pores having curved edges above the height of film surface (Fig. 4A). Due to the high edges of these craters, the FLM_{CHI/H_M} films showed a high R_a value that is the second highest among those of all films. The images of FLM_{CHI-CP/H_M} films clearly showed how the addition of CP caused the rough flat film surface of FLM_{CHI/H_M} to turn into a wavy surface showing the highest R_a value (Fig. 4B). The addition of EUG into films reduced their wavy nature, and caused a dramatic reduction in films roughness (lowest R_a among those of films obtained by H_M), but this also caused formation of extensive tiny pores at the film surface (Fig. 4C). These pores observed confirms that the EUG could not be emulsified effectively by H_M and part of the EUG separated as EO droplets evaporated during drying of films. The topographic images of FLM_{CHI/H_M-H_{US}} films showed that H_M-H_{US} treatment caused a much wavy CHI film surface than that of FLM_{CHI/H_M} (Fig. 4D). Moreover, FLM_{CHI-CP/H_M-H_{US}} film surface also became much rougher than that of FLM_{CHI-CP/H_M} (Fig. 4E). It is also important to note that the H_M-H_{US} treatment caused significant reductions in R_a of films. The surface images of FLM_{CHI-CP-EUG/H_M-H_{US}} film showed that addition of EUG reduced the roughness and R_a of films as observed similarly in FLM_{CHI-CP-EUG/H_M} films (Fig. 4F). However, extensive crater-like pores observed at the FLM_{CHI-CP-EUG/H_M} film surface disappeared in FLM_{CHI-CP-EUG/H_M-H_{US}} films. Thus, both SEM and AFM images of films confirmed that the US is an effective method to emulsify EUG and prevent pore formation at the film surface due to evaporation of unemulsified EO droplets accumulated at the film surface before cast films dried.

3.4. Effect of US and CP compositing on optical properties and color of films

The effects of US treatment on UV light transmittance at 280 nm (T₂₈₀) and VIS light transmittance at 600 nm (T₆₀₀), opacity and color change (ΔE*) of films are presented in Table S4 (see Supplementary file). The application of H_M-H_{US} in film preparation caused a significantly lower T₂₈₀ for pristine CHI films than application of H_M. It seems that the US caused some molecular modifications such as linearization of folded CHI molecules that might expose UV-absorbing N-acetylglucosamine residues (Kasaai, 2009). The formation of composites with CP and the addition of EUG caused further significant reductions in T₂₈₀ due to additional UV-absorbing aromatic amino acid residues and aromatic ring of these molecules, respectively, but no significant differences exist between H_M-H_{US} and H_M treated EUG incorporated CHI or CHI-CP films. As expected, CHI films showed a higher T₆₀₀ and lower opacity than CHI-CP composites. Moreover, incorporation of EUG caused a reduction in T₆₀₀ of films, possibly by the effect of emulsion formation in the presence of essential oil by H_M-H_{US} or H_M. The application of H_M-H_{US} in film preparation caused a significantly lower T₆₀₀ for CHI-CP films than application of H_M, but no differences exist between T₆₀₀ values of CHI

Table 2

Tensile strength, elongation at break, Young's modulus and toughness of different films^{a,b}.

Samples	TS (MPa)	EB (%)	YM (MPa)	T (MPa)
FLM _{CHI/H_M}	3.54 ± 0.38 ^d	92.12 ± 4.70 ^a	0.02 ± 0.001 ^f	129.33 ± 16.37 ^e
FLM _{CHI/H_M-H_{US}}	4.24 ± 0.67 ^d	17.69 ± 2.07 ^d	0.21 ± 0.02 ^a	36.70 ± 8.19 ^f
FLM _{CHI-CP/H_M}	6.62 ± 1.00 ^c	81.75 ± 5.92 ^b	0.04 ± 0.005 ^{de}	235.74 ± 41.62 ^c
FLM _{CHI-CP/H_M-H_{US}}	11.50 ± 0.85 ^a	61.32 ± 3.03 ^c	0.15 ± 0.01 ^b	321.51 ± 29.06 ^b
FLM _{CHI-EUG/H_M}	6.06 ± 1.08 ^c	83.54 ± 5.47 ^b	0.03 ± 0.01 ^e	190.19 ± 36.83 ^d
FLM _{CHI-EUG/H_M-H_{US}}	5.77 ± 0.38 ^c	63.46 ± 2.80 ^c	0.05 ± 0.01 ^d	149.27 ± 11.88 ^e
FLM _{CHI-CP-EUG/H_M}	10.05 ± 1.05 ^b	82.91 ± 7.86 ^b	0.07 ± 0.01 ^c	339.81 ± 52.56 ^b
FLM _{CHI-CP-EUG/H_M-H_{US}}	11.80 ± 1.34 ^a	91.68 ± 3.77 ^a	0.07 ± 0.01 ^c	418.41 ± 50.17 ^a

^a Different lower letter superscripts in the same column indicate significant difference ($P < 0.05$).

^b Values are presented as mean value ± SD (n = 10).

films obtained by different methods. It seems that the reduced T₆₀₀ in CHI-CP films by application of US treatment occurred due to the increased CP solubility and distribution within the film matrix. In general, a reduced T₆₀₀ caused parallel increases in film opacity. Moreover, incorporation of EUG in CHI films caused increased yellowness (see b* values and film photos in Supplementary file Table S5 and Fig. S6, respectively), but this caused minimum color change in CHI-CP composite films.

3.5. Effect of US and CP compositing on water vapor permeability of edible films

The results of water vapor permeability (WVP) measurements for CHI and CHI-CP composite films produced by H_M or H_M-H_{US} treatments were also presented in Table 1. The similar WVP values of FLM_{CHI/H_M} and FLM_{CHI/H_M-H_{US}} films showed that the application of US did not affect the WVP of CHI films. The similar WVPs of FLM_{CHI-EUG/H_M} and FFS_{CHI-EUG/H_M-H_{US}} also showed that the addition of EUG into CHI films by H_M or H_M-H_{US} did not also affect the WVP. The FLM_{CHI-CP/H_M} and FLM_{CHI-CP/H_M-H_{US}} films also showed a similar WVP to all other CHI films with the exception of FLM_{CHI-CP/H_M-H_{US}} film that showed significantly lower WVP than FLM_{CHI/H_M} film. However, the FLM_{CHI-CP-EUG/H_M-H_{US}} film showed the lowest WVP of the current study, indicating that the use of CP and EUG, and the application of US are the key factors causing a significant improvement in WVP of composite films. It appears that the improved WVP of films might be due to the effect of multiple US-mediated factors such as the formation of denser film morphology by effective solubilization of CP, increased film tortuosity by the distributed EUG droplets emulsified by CP, and pore free nature of films due to lack of unemulsified EUG droplets.

3.6. Effects of US and CP compositing on mechanical properties of edible films

The mechanical properties of CHI and CHI-CP composite films are displayed in Table 2. The US-treatment did not significantly affect the TS values of pristine CHI films and CHI films incorporated with EUG, but it caused a reduction of EB and T values, and an increase in YM values of these films. The reduced EB, but increased YM of US-treated CHI films suggested that the sonication applied in film-making caused increase of film stiffness and reduction of CHI biopolymers' mobility within the film matrix. Moreover, reduction of T values of films by US-treatment suggested that the sonication caused some degradation of CHI biopolymer resulting in a reduction of its chain length as observed also by Rokita,

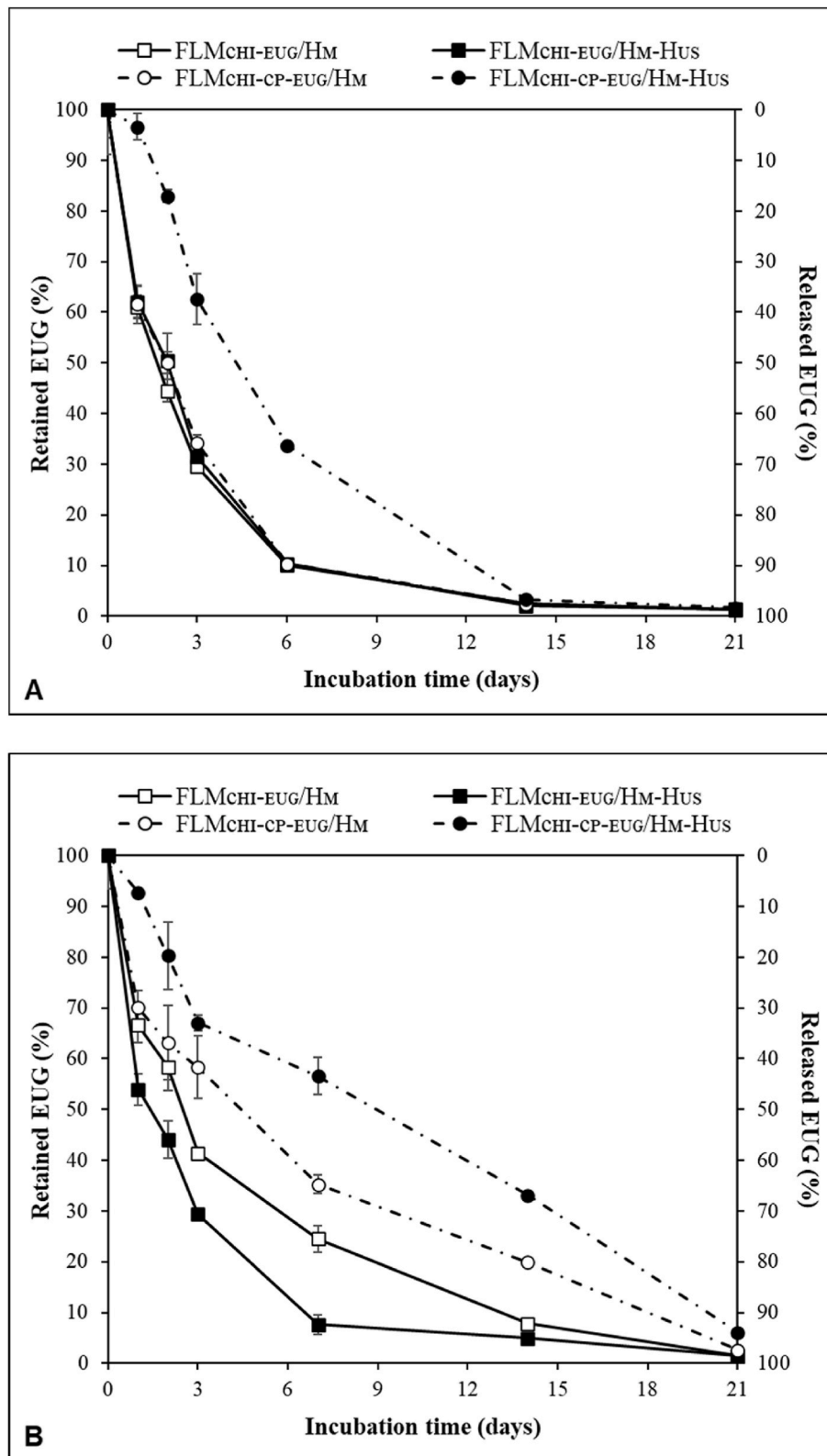


Fig. 5. EUG retention in different CHI and CHI-CP composite films incubated at room temperature (A) and refrigerated storage temperature at 10 °C (B).

Czechowska-Biskup, Ulanski, and Rosiak (2005). It is important to note that the incorporation of EUG caused significant increases in TS and T of CHI films treated with H_M or H_M-H_{US} . These results suggested increased interaction among CHI biopolymers, possibly due to cross-linking effect of EUG. In the literature, ability of EUG to participate cross-linking of zein film matrix has been reported by Khalil, Deraz, Elrahman, and

El-Fawal (2015). The mechanical test results of CHI-CP films showed that all composites showed significantly higher TS and T than their corresponding CHI films. This finding clearly showed that the composite films owe their mechanical stability to interactions and networking formed between CHI and CP. It is also important to note that $FLM_{CHI-CP-EUG}/H_M-H_{US}$ and FLM_{CHI-CP}/H_M-H_{US} films showed

Table 3

The first-order rate constant (k), half-life ($T_{1/2}$), and correlation coefficient (R^2) of EUG loss following exposure of films to air at room temperature (T_R) and or at 10 °C.

Samples		k (day ⁻¹)	$T_{1/2}$ (day)	R^2
T_R	FLM _{CHI-EUG/H_M}	0.38	1.8	0.9973
	FLM _{CHI-EUG/H_M-H_{US}}	0.37	1.9	0.9952
	FLM _{CHI-CP-EUG/H_M}	0.37	1.9	0.9939
	FLM _{CHI-CP-EUG/H_M-H_{US}}	0.19	3.6	0.9705
10 °C	FLM _{CHI-EUG/H_M}	0.17	4.0	0.9828
	FLM _{CHI-EUG/H_M-H_{US}}	0.21	3.3	0.8895
	FLM _{CHI-CP-EUG/H_M}	0.11	6.5	0.9639
	FLM _{CHI-CP-EUG/H_M-H_{US}}	0.08	9.1	0.9749

Table 4

Percentage of soluble EUG^a in films determined by release tests in aqueous and fatty food simulants at 4 °C and 25 °C^{b,c}.

Samples	Aqueous food simulant (simulant A) ^d		Fatty food simulant (simulant D1) ^e	
	4 °C	25 °C	4 °C	25 °C
FLM _{CHI-EUG/H_M}	51.9 ± 4.1 ^c	56.4 ± 3.8 ^b	54.4 ± 4.0 ^b	55.3 ± 1.9 ^{bc}
FLM _{CHI-EUG/H_M-H_{US}}	53.9 ± 1.1 ^{bc}	55.6 ± 1.2 ^b	48.1 ± 1.0 ^c	50.1 ± 1.3 ^c
FLM _{CHI-CP-EUG/H_M}	57.3 ± 3.3 ^b	58.8 ± 16.6 ^b	58.3 ± 6.2 ^{ab}	57.2 ± 3.8 ^b
FLM _{CHI-CP-EUG/H_M-H_{US}}	66.8 ± 1.4 ^a	71.35 ± 6.03 ^a	60.9 ± 1.7 ^a	70.0 ± 8.1 ^a

^a Soluble EUG (%) = (EUG_{max}/EUG_{incorporated}) × 100. ^b Different lower letter superscripts in the same column indicate significant difference ($P < 0.05$). ^c Values are presented as mean value ± SD (n = 6). ^d The equilibrium point of release was reached at 24 h. ^e The equilibrium point of release was reached at 44 h.

significantly higher EB than FLM_{CHI-EUG/H_M-H_{US}} and FLM_{CHI/H_M-H_{US}} films, respectively. In contrast, the application of H_M alone did not give CHI-CP films having superior EB values than those of CHI films. Thus, it seems that the solubilization of CP by US treatment maximized film flexibility by preventing formation of insoluble protein aggregates that disrupt the continuity of the film matrix.

3.7. Release kinetics of EUG from edible films exposed to air

The ability of edible antimicrobial films to retain essential oils during storage is a major factor affecting the shelf-life of coated or packaged foods. Therefore, release profiles of EUG from films to air are estimated by determining the remaining EUG in films exposed to air at room temperature (T_R) or refrigerated storage temperature at 10 °C (Fig. 5A and B). Fig. 5A clearly showed that FLM_{CHI-EUG/H_M}, FLM_{CHI-EUG/H_M-H_{US}}, and FLM_{CHI-CP-EUG/H_M} films showed a rapid release of EUG to air at T_R . In contrast, FLM_{CHI-CP-EUG/H_M-H_{US}} film showed a high retention of EUG at T_R indicating superior sustained release properties of these films than all others. For example, it should be noted that the FLM_{CHI-CP-EUG/H_M-H_{US}} films lost only 3% EUG within 1 day at T_R while it took 3 days at T_R to lost 38% of EUG from these films. However, all other films lost almost 38% of their initial EUG content within 1 day at T_R . The reduction of release temperature to 10 °C reduced the release rates of EUG for all films. However, FLM_{CHI-EUG/H_M-H_{US}} was still having the lowest release rates for the EUG at 10 °C. The fitting of the obtained retention data to first-order reaction kinetics (see Table 3 and Supplementary file, Figs. S7A and B) revealed that the half-life ($T_{1/2}$) for EUG loss in FLM_{CHI-CP-EUG/H_M-H_{US}} film exposed to air at T_R was 3.6 days while other films' $T_{1/2}$ values changed between 1.8 and 1.9 days at T_R . The $T_{1/2}$ of FLM_{CHI-CP-EUG/H_M-H_{US}} at 10 °C was also 2.3-, 2.8-, 1.4-fold greater than those of FLM_{CHI-EUG/H_M}, FLM_{CHI-EUG/H_M-H_{US}}, FLM_{CHI-CP-EUG/H_M}, respectively. These results clearly proved that application of H_M-H_{US} is highly

Table 5

Sprouting rate of bulbs during storage at room temperature.

Samples ^d	Storage time (days)					
	0	1	7	14	21	28
Control (uncoated)	0/10	0/10	2/10	4/10	4/10	3/10
FLM _{CHI/H_M-H_{US}}	0/10	0/10	0/10	4/10	4/10	4/10
FLM _{CHI-CP/H_M-H_{US}}	0/10	0/10	0/10	3/10	3/10	2/10
FLM _{CHI-CP-EUG/H_M}	0/10	0/10	0/10	2/10	4/10	2/10
FLM _{CHI-CP-EUG/H_M-H_{US}}	0/10	0/10	0/10	1/10	1/10	1/10

^a Different batches (10 bulbs) of bulbs were examined daily to count number of sprouted bulbs.

beneficial to obtain CHI-CP composite films with sustained EUG release properties. It appears that the CHI-CP complex is an effective formation to encapsulate emulsified EUG and form a dense barrier against its loss by evaporation. It is also important to note that even FLM_{CHI-CP-EUG/H_M} showed higher $T_{1/2}$ than FLM_{CHI-EUG/H_M} and FLM_{CHI-EUG/H_M-H_{US}} at 10 °C. It is evident that H_M or H_M-H_{US} has no considerable effect on EUG retention performance of pristine CHI films. It is clear that the CHI molecules and conformational formations in the film matrix lack ability to interact and encapsulate the EUG effectively.

3.8. Determination of soluble EUG content of edible films released in different food simulants

The results of soluble EUG contents of films determined by release tests performed in standard aqueous (simulant A: ethanol at 10%, v/v) and fatty (simulant D1: ethanol at 50%, v/v) food simulants until reaching of equilibrium at 4 °C and 25 °C are presented in Table 4 (see release curves in Supplementary file, Figs. S8 and S9). As expected, the percentage of soluble EUG released from most films at 25 °C was slightly to moderately higher than that released at 4 °C. This was expected since elevated temperature might have increased the tendency of emulsions to destabilize and release emulsified EUG, or it increased diffusion of entrapped EUG within macromolecular formations or complexes. It is only the FLM_{CHI-CP-EUG/H_M} film that showed almost same amounts of EUG release at 4 °C and 25 °C in the fatty food simulant. Thus, it seems that the large amounts of insoluble CP aggregates in FLM_{CHI-CP-EUG/H_M} film adsorbed or entrapped part of the soluble EUG with high affinity and prevented its release at elevated temperature. It should also be noted that the amounts of EUG released in aqueous and fatty food simulants by films were not considerably different from each other, but reaching of equilibrium in the aqueous simulant occurred much faster (24 h) than that in the fatty simulant (44 h) due possibly differences in EUG solubility and film swelling profiles of simulants. The similar amounts of EUG released in different simulants, originate possibly from amphiphilic nature of this EO, suggest its suitability as a preservative compound for a great variety of food products. These results showed that CHI films prepared by H_M or H_M-H_{US} maintained slightly more than half of their initially incorporated EUG in soluble form. It seems that the remaining EUG incorporated into films lost by evaporation during initial drying period of films. The release tests of CHI-CP composite films clearly showed that these films prepared by H_M or H_M-H_{US} showed higher amounts of soluble EUG than corresponding CHI films. It is important to note that FLM_{CHI-CP-EUG/H_M-H_{US}} film showed the highest amount of soluble EUG that is almost 28 and 40% higher than those of FLM_{CHI-EUG/H_M-H_{US}} films in simulant A and D1, respectively. It is clear that the surface active CP and its complexes with CHI helped retention of EUG by encapsulating this EO via physical trapping and/or emulsification and preventing its evaporation during film-drying. It is also clear that use of CP in composite-making and US-treatment helped retaining minimum 70% of incorporated EUG in soluble form.

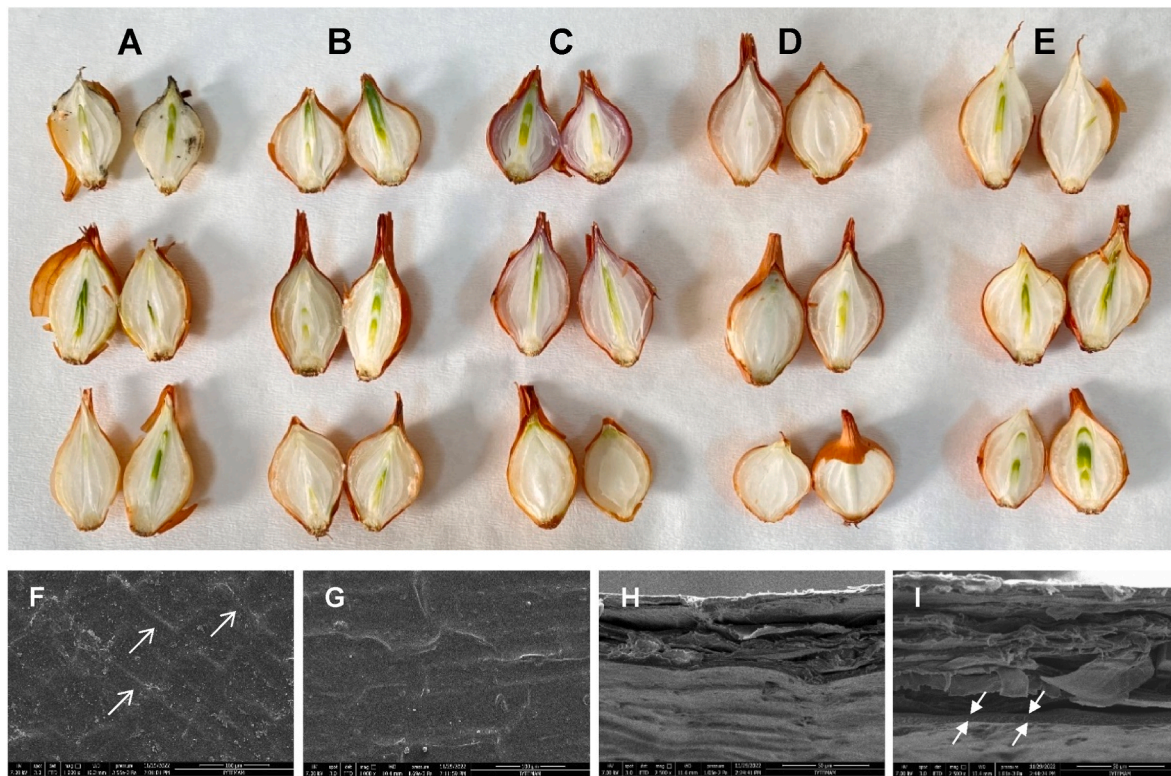


Fig. 6. Cross-section photos of onion bulbs after 2-weeks storage at room temperature [(uncoated control onions (A), onions coated with FLM_{CHI}/H_M-H_{US} (B), FLM_{CHI-CP}/H_M-H_{US} (C), FLM_{CHI-CP-EUG}/H_M-H_{US} (D), FLM_{CHI-CP-EUG}/H_M (E)]; SEM surface and cross-section images of active composite coating at onion skins [surface of uncoated onion skin (F), and onion skin coated with FLM_{CHI-CP-EUG}/H_M-H_{US} (G); cross-section of uncoated onion skin (H), and onion skin coated with FLM_{CHI-CP-EUG}/H_M-H_{US} (I); arrows indicate coating layer].

Table 6
Green color strength of developed sprouts.

Samples	Green color strength ^d			
	1	2	3	4
Control (uncoated)	–	–	4/10	6/10
FLM _{CHI} /H _M -H _{US}	–	–	2/10	8/10
FLM _{CHI-CP} /H _M -H _{US}	–	–	8/10	2/10
FLM _{CHI-CP-EUG} /H _M -H _{US}	–	–	5/10	5/10
FLM _{CHI-CP-EUG} /H _M	1/10	4/10	4/10	1/10

^a 1: white; 2: yellow; 3: yellowish green; 4: green.

3.9. Performance of developed composite edible films as active coating for stored onions

3.9.1. Antisprouting effect of active composite coating for stored onions

The effect of developed composite coating on sprouting, the greatest physiological problem causing decay in stored bulbs, have been tested by examination of sprouting rate during storage at room temperature (Table 5). Each time-point represents the result for a different party of onions since the bulbs were cut and analyzed for internal details each time (Fig. 6). At the first week of storage, the coated onions did not show any sprouting while sprouting was observed in some uncoated control onions (2 sprouted in 10 bulbs). The uncoated control onions and onions coated with FLM_{CHI}/H_M-H_{US} showed considerable sprouting after 2 weeks (Fig. 6A and B). In fact, 3–4 sprouted onions were observed in every 10 bulbs of these samples between 2 and 4 weeks. The onions coated with FLM_{CHI-CP}/H_M-H_{US} films showed slightly less sprouting within 4-weeks period (2–3 sprouted in 10 bulbs) (Fig. 6C). However, the use of FLM_{CHI-CP-EUG}/H_M-H_{US} films in coating caused the most

marginal drop in number of sprouted onions (1 sprouted in 10 bulbs) between 2 and 4 weeks (Fig. 6D). In contrast, the use of FLM_{CHI-CP-EUG}/H_M films that caused poor EUG retention capacity caused 2–4 sprouting in 10 onions during 28-days storage (Fig. 6E). Moreover, the FLM_{CHI-CP-EUG}/H_M coating showed a similar effectiveness with FLM_{CHI-CP}/H_M-H_{US} coatings. Thus, it is clear that the amount of EUG left in coatings prepared by H_M during storage was ineffective on inhibition of sprouting.

The green color strength of developed sprouts was also evaluated for uncoated control and different coated bulbs at the end of 28 days as a measure of strong sprouting (Table 6). The sprouts of uncoated control bulbs, and those of FLM_{CHI}/H_M-H_{US}, FLM_{CHI-CP}/H_M-H_{US}, and FLM_{CHI-CP-EUG}/H_M coated bulbs were yellowish-green or green while sprouts of FLM_{CHI-CP-EUG}/H_M-H_{US} coated bulbs were yellow or yellowish-green. This result showed beneficial effect of FLM_{CHI-CP-EUG}/H_M-H_{US} coating to delay accumulation of chlorophyll in sprouts formed by onions. In contrast, the sprouts of bulbs coated with FLM_{CHI-CP-EUG}/H_M had a yellowish-green or green color very similar to those of uncoated bulbs. These results were in line with those of sprouting rates, and they confirmed that the FLM_{CHI-CP-EUG}/H_M-H_{US} coatings were effective to suppress development of sprouting in onions.

The solution-cast films of FLM_{CHI}/H_M-H_{US} and FLM_{CHI-CP-EUG}/H_M-H_{US}, the worst and best performed coatings of these films in anti-sprouting test, respectively, did not show considerably different oxygen permeability values (28.07 ± 3.33 g mm/m².day for former and 27.94 ± 4.58 g mm/m².day for latter films). Therefore, it is not likely that the differences in the sprouting rate of onions were mediated by oxygen permeability characteristics of coatings. It is clear that the FLM_{CHI-CP-EUG}/H_M-H_{US} coating owed its effectiveness to its high retention capacity of EUG that is a well-known natural antisprouting agent (Finger et al., 2018; Kleinkopf et al., 2003; Santos et al., 2020).

3.9.2. Effect of active composite coating on physicochemical properties of stored onions

The effect of active coating on pH, titratable acidity (TA) and brix ($^{\circ}\text{Bx}$) of coated onions are presented in Tables S6–S8 (see Supplementary file). The storage caused some limited drops in pH and TA of both uncoated and coated bulbs due possibly to some reduction of acids (mainly citric acid and malic acid) by respiration. It was reported that the storage temperature was the most important factor influencing the acid changes (e.g., citric acid increases and malic acid decreases) in bulbs especially at high storage temperatures near 30 °C (Salama, Hicks, and Nock, 1990). At 1st and 28th days of storage, the pHs and TAs of uncoated control onions were 5.81 and 5.66, and 0.27 and 0.21 g MA/100 g f.w. while coated onions showed pHs and TAs of 5.82–5.88 and 5.71–5.76, and 0.27–0.30 and 0.21–0.24 g MA/100 g f.w., respectively. The $^{\circ}\text{Bx}$ values of uncoated and coated onions changed between 13.5 and 15.3, and 13.2 and 15.8 during 28-days storage, respectively. No significant differences were observed among $^{\circ}\text{Bx}$ of uncoated and coated onion samples. Most samples also did not show a significant change in their $^{\circ}\text{Bx}$ during storage, except significant increases in $^{\circ}\text{Bx}$ values of uncoated bulbs at the 3rd week, and bulbs coated with FLM_{CHI}/H_M-H_{US} at the 2nd week. The uncoated bulbs maintained their increased $^{\circ}\text{Bx}$ at the 4th week while FLM_{CHI}/H_M-H_{US} coated bulbs showed a rapid decline in their $^{\circ}\text{Bx}$ at the 4th week. The increase of $^{\circ}\text{Bx}$ in onions is sometimes linked with onset of sprouting while following decline in $^{\circ}\text{Bx}$ is linked with metabolic activity of growing sprout (Hurst, Shewfelt, & Schuler, 1985; Marković et al., 2020; Sheikh, Jose-Santhi, Kalia, Singh, & Singh, 2022). These results showed high parallelism with our findings since uncoated and FLM_{CHI}/H_M-H_{US} coated bulbs showed highest sprouting rate and greenest sprout color in our examinations.

3.9.3. Effect of active composite coating on firmness of stored onions

The firmness of onions determined both on their root-end and equatorial regions are provided in Tables S9 and S10 (see Supplementary file), respectively. At the 1st day of storage, coated bulbs showed slightly to moderately or considerably greater firmness than uncoated control bulbs at the root-end and equatorial regions, respectively. All bulbs showed a significant increase in root-end or equatorial region firmness starting from 1st week by the effect of drying occurred at their skins and 1st scales. However, the increases in the firmness of equatorial regions were considerably greater than those at the root-ends. No significant differences were determined among the root-end firmness of uncoated and coated bulbs between 1st and 4th weeks of storage. However, most coated bulbs showed a greater equatorial region firmness than uncoated controls between 1st and 4th weeks. It appears that the applied CHI and CHI-CP coatings increased the integrity of onion skins by acting as a flexible supporting layer.

3.9.4. SEM surface and cross-section images of active composite coating at onion skins

The application of coatings caused tight packing of skin and 1st scale of onions, thus, this effectively prevented cracking and disintegration of dried skins. The SEM photos of the skin surface of uncoated and FLM_{CHI-CP-EUG}/H_M-H_{US} coated onions clearly showed that the developed active composite coating effectively covered the skin surface and increased its smoothness (Fig. 6F and G). Although the skin outer surface was masked by a cuticle layer, the cell-walls at the uncoated onion skin are somehow identifiable (see arrows in Fig. 6F). In contrast, cell-walls in the surface micrographs of FLM_{CHI-CP-EUG}/H_M-H_{US} coated onion skin were hardly identifiable confirming the presence of composite coating at the surface. The thicknesses of the onion skin and FLM_{CHI-CP-EUG}/H_M-H_{US} coating on the skin determined from SEM cross-section photos were 45 and 4.5 μm , respectively. No apparent changes were observed in the morphologies of highly plated inner layers of coated and uncoated onion skins (Fig. 6H and I).

Table 7

Effects of antimicrobial coatings on *L. innocua* and *E. coli* counts of inoculated bulbs stored at room temperature.

Microorganism	Coatings	Storage time (days) ^{a,b}			
		Day 0 ^d	Day 1	Day 5	
<i>L. innocua</i> (Log cfu/g) ^c	Control (uncoated)	5.8 ± 0.41 ^{b,A}	7.1 ± 0.07 ^{b,A}	7.0 ± 0.30 ^{b,A}	
	FLM _{CHI} /H _M -H _{US}	4.7 ± 0.13 ^{a,B}	4.6 ± 0.12 ^{ab,B}	4.5 ± 0.07 ^{b,C}	
	FLM _{CHI-CP} /H _M -H _{US}	4.1 ± 0.20 ^{c,C}	4.5 ± 0.05 ^{b,B}	5.0 ± 0.19 ^{a,B}	
	FLM _{CHI-EUG} /H _M -H _{US}	<2.0 ^{c,D}	3.6 ± 0.10 ^{b,C}	3.8 ± 0.18 ^{a,D}	
	FLM _{CHI-CP-EUG} /H _M -H _{US}	<2.0 ^{c,D}	2.8 ± 0.12 ^{b,D}	3.2 ± 0.09 ^{a,E}	
	<i>E. coli</i> (Log cfu/g) ^c	Control (uncoated)	4.6 ± 0.30 ^{a,A}	5.1 ± 0.36 ^{b,A}	5.5 ± 0.76 ^{a,A}
	FLM _{CHI} /H _M -H _{US}	4.4 ± 0.20 ^{a,A}	4.3 ± 1.13 ^{a,A}	4.1 ± 0.80 ^{a,B}	
	FLM _{CHI-CP} /H _M -H _{US}	3.8 ± 1.00 ^{a,B}	4.2 ± 1.49 ^{a,A}	5.0 ± 0.50 ^{a,A}	
	FLM _{CHI-EUG} /H _M -H _{US}	<2.0 ^{b,C}	<2.0 ^{b,B}	3.4 ± 0.48 ^{a,BC}	
	FLM _{CHI-CP-EUG} /H _M -H _{US}	<2.0 ^{b,C}	<2.0 ^{b,B}	2.7 ± 0.65 ^{a,C}	

^a Different lower and capital letter superscripts in the same row and column indicate significant differences ($P < 0.05$), respectively.

^b Values are presented as mean value ± SD ($n = 6$).

^c Initial *L. innocua* or *E. coli* loads were 8.7 log cfu/mL.

^d Bacterial load after 15 min when coated onions were still wet.

3.9.5. Antimicrobial effect of active composite coating on inoculated stored onions

The results showing the antimicrobial effect of CHI and CHI-CP coatings with or without EUG on *L. innocua* inoculated onto the surface of bulbs prior to coating are presented in Table 7. The ability of inoculated *L. innocua* to grow on to the surface of uncoated control onions (increased > 1 log) during room storage showed that the test bacteria survived on inoculation surface. The *L. innocua* counts of all coated bulbs were significantly lower than that of uncoated control bulbs on the 0th day when coatings were initially wet, and on the 1st and 5th days after drying of coating ($P < 0.05$). The antimicrobial effect of coatings lacking EUG on *L. innocua* showed that both the pristine CHI and CHI-CP composite films had antimicrobial effects on inoculated bacteria. It is interesting to report that the wet FLM_{CHI-CP}/H_M-H_{US} coating showed significantly higher antilisterial effect than wet FLM_{CHI}/H_M-H_{US} coating on the 0th day. The dried FLM_{CHI}/H_M-H_{US} and FLM_{CHI-CP}/H_M-H_{US} coatings showed similar antilisterial effects on the 1st day of storage, but the former showed significantly higher antimicrobial effect than the latter on the 5th day of storage ($P < 0.05$). This result was expected since CP probably blocked some reactive amino groups of CHI in composite films by complexation, but it is evident that the developed CHI-CP films still showed some significant inherent antimicrobial activity. The incorporation of EUG into CHI and CHI-CP coatings boosted their antimicrobial activity and caused a minimum 3.8 log lower *Listeria* counts in coated onions than in uncoated onions on the 0th day (wet coatings). The onions coated with FLM_{CHI-EUG}/H_M-H_{US} and FLM_{CHI-CP-EUG}/H_M-H_{US} also showed minimum 3 log lower *Listeria* counts than uncoated inoculated onions on the 1st and 5th days (dried coatings). However, it is important to note that FLM_{CHI-CP-EUG}/H_M-H_{US} coating gave significantly lower *Listeria* counts than FLM_{CHI-EUG}/H_M-H_{US} coating ($P < 0.05$) owing to its higher EUG retention capacity during storage.

The antimicrobial effect of CHI and CHI-CP coatings on *E. coli* inoculated onto surface of bulbs prior to coating are also presented in Table 7. The *E. coli* inoculated onto surface of control uncoated onions showed no inactivation during 5-days room storage. The bacteria initially showed a resistance against FLM_{CHI}/H_M-H_{US}, immediately after coating on the 0th day (wet coating) and after 1-day storage (dry

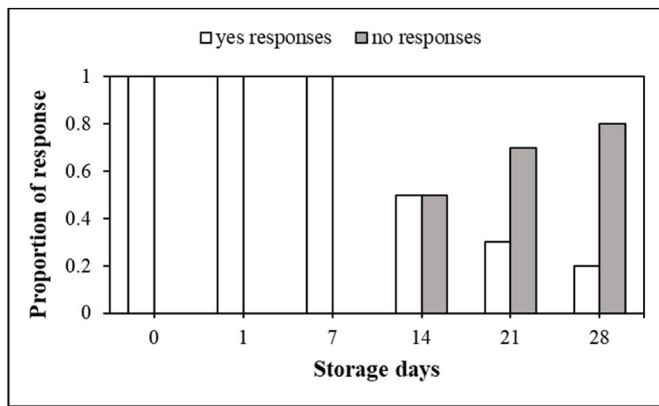


Fig. 7. The results of sensory test showing proportions of yes/no responses for detection of EUG odor.

coating) and showed no considerable inactivation, but the coating caused significant inactivation of *E. coli* after 5-days storage. In contrast, FLM_{CHI-CP}/H_M-H_{US} caused a significant reduction in *E. coli* counts initially on the 0th day (wet films), but did not cause further significant inactivation of *E. coli* during 5-days storage. Similar to *Listeria*, *E. coli* also showed a considerable inactivation when EUG was incorporated into coatings. The FLM_{CHI-EUG}/H_M-H_{US} and FLM_{CHI-CP-EUG}/H_M-H_{US} coatings caused a minimum 2.6 log reduction of *E. coli* counts on the 0th day, and kept *E. coli* counts of onions 2.1 and 2.8 log lower than those of uncoated controls at the end of 5-days, respectively. Although FLM_{CHI-CP-EUG}/H_M-H_{US} coating was slightly more effective than FLM_{CHI-EUG}/H_M-H_{US} coating on *E. coli*, the differences between antimicrobial activity of two films were not significant ($P > 0.05$).

3.9.6. End-point sensory test for detection of EUG in coated onions during storage

The sensory tests conducted to detect EUG originated odor difference between uncoated and FLM_{CHI-CP-EUG}/H_M-H_{US} coated onions were evaluated by determining “yes” and “no” responses for a paired comparison test (Fig. 7). According to results, the inherent clove-like smell of EUG in FLM_{CHI-CP-EUG}/H_M-H_{US} coated onions was detected by all panelist after 1-week storage. The EUG odor of coated onions was still detected by half of the panelists after 2 weeks, but it has not been detected by 80% of the panelists after 28 days.

4. Conclusions

The poor surface activity of chitosan is a major problem causing rapid loss of incorporated volatile essential oils into its edible films intended for antimicrobial food packaging. The current work clearly showed that the unique inherently antimicrobial edible packaging material chitosan could be used more effectively in antimicrobial coating by using its composites with surface active chickpea proteins. The major beneficial effect of chickpea proteins originated from their essential oil encapsulation and/or emulsification capacity that enhances the retention of essential oil in film-forming solutions and in dried films, and enables its sustained release from packaging on to air or food surface during storage. The composite structure also provides better mechanical and moisture barrier properties than those of pristine chitosan films. However, the use of ultrasonic homogenization is the key process necessary to obtain desired composites since it effectively solubilize chickpea proteins and emulsify incorporated essential oil. Most of the benefits of composite structure, except improved mechanical properties, could not be obtained when ultrasonic homogenization is replaced by mechanical homogenization during incorporation of EUG. The test of performances of eugenol incorporated composite films on onions as coating showed that the developed coating inhibited contaminated

gram-negative and positive pathogenic bacteria, and delayed sprouting of coated onions more effectively than pristine eugenol incorporated chitosan coatings. Tests with coatings free from eugenol showed that a considerable portion of inherent antimicrobial activity of chitosan is maintained in the composite films suggesting availability of most amino groups of this polysaccharide after interaction with chickpea proteins. This work opened a new perspective in more effective use of chitosan as essential oil loaded antimicrobial packaging by forming its composites with sustainable chickpea proteins.

CRedit authorship contribution statement

Pelin Barış Kavur: Conceptualization, Data curation, Investigation, Methodology, Writing – original draft. **Ahmet Yemencioğlu:** Conceptualization, Methodology, Project administration, Supervision, Writing – review & editing.

Declaration of competing interest

The authors declare that they have no known competing financial interests or personal relationships that could have appeared to influence the work reported in this paper.

Data availability

Data will be made available on request.

Acknowledgement

We thank Integrated Research Center (TAM) at Izmir Institute of Technology for ζ-potential, fluorescence microscopy, SEM and AFM analyses, and Central Research Laboratories (MERLAB) at Izmir Katip Celebi University for particle size analysis.

Appendix A. Supplementary data

Supplementary data to this article can be found online at <https://doi.org/10.1016/j.foodhyd.2024.109790>.

References

- Alkan, D., & Yemencioğlu, A. (2006). Potential application of natural phenolic antimicrobials and edible film technology against bacterial plant pathogens. *Food Hydrocolloids*, 55, 1–10. <https://doi.org/10.1016/j.foodhyd.2015.10.025>
- Almeida, De, J.M., Crippa, B. L., de Souza, V. V. M. A., Alonso, V. P. P., Júnior, E. D. M. S., & Picone, C.S.F., Prata, A.S., & Silva, N.C.C. (2023). Antimicrobial action of oregano, thyme, clove, cinnamon and black pepper essential oils free and encapsulated against foodborne pathogens. *Food Control*, 144(109356). <https://doi.org/10.1016/j.foodcont.2022.109356>
- AOAC. (2000). Official method 942.15 acidity (titratable) of fruit products. *Official Methods of Analysis of AOAC International*.
- Ariyaratna, I. R., & Karunaratne, D. N. (2016). Microencapsulation stabilizes curcumin for efficient delivery in food applications. *Food Packaging and Shelf Life*, 10, 79–86. <https://doi.org/10.1016/j.foodps.2016.10.005>
- ASTM. (1995). E96–95 Standard test methods for water vapor transmission of materials. *ASTM International*.
- ASTM. (2002). D882–02 Standard test method for tensile properties of thin plastic sheeting. *ASTM International*.
- Atli, O., Karaca, A. C., & Ozelcik, B. (2023). Encapsulation of cumin (*Cuminum cyminum* L.) seed essential oil in the chickpea protein-maltodextrin matrix. *ACS Omega*, 8, 4156–4164. <https://doi.org/10.1021/acsomega.2c07184>
- Ayala-Zavala, J. F., González-Aguilar, G. A., & Del-Toro-Sánchez, L. (2009). Enhancing safety and aroma appealing of fresh-cut fruits and vegetables using the antimicrobial and aromatic power of essential oils. *Journal of Food Science*, 74(7), R84–R91. <https://doi.org/10.1111/j.1750-3841.2009.01294.x>
- Aydemir, L. Y., & Yemencioğlu, A. (2013). Potential of Turkish Kabuli type chickpea and green and red lentil cultivars as source of soy and animal origin functional protein alternatives. *LWT - Food Science and Technology*, 50, 686–694. <https://doi.org/10.1016/j.lwt.2012.07.023>
- Bradford, M. M. (1976). A rapid and sensitive method for the quantitation of microgram quantities of protein utilizing the principle of protein-dye binding. *Analytical Biochemistry*, 72, 248–254. [https://doi.org/10.1016/0003-2697\(76\)90527-3](https://doi.org/10.1016/0003-2697(76)90527-3)

- CDC (Centers of Disease Control and Prevention). (2016). Multistate outbreak of Listeriosis linked to Frozen vegetables (final update). <https://www.cdc.gov/listeria/outbreaks/frozen-vegetables-05-16/index.html> Accessed August 2023.
- CDC (Centers of Disease Control and Prevention). (2020). "Outbreak of *Salmonella* Newport infections linked to onions." <https://www.cdc.gov/salmonella/newport-07-20/index.html>.
- CDC (Centers of Disease Control and Prevention). (2021). *Salmonella* outbreak linked to onions. <https://www.cdc.gov/salmonella/oranienburg-09-21/index.html>.
- Chen, Y., Liu, Y., Dong, Q., Xu, C., Deng, S., Kang, Y., et al. (2023). Application of functionalized chitosan in food: A review. *International Journal of Biological Macromolecules*, 235(123716). <https://doi.org/10.1016/j.ijbiomac.2023.123716>
- Clegg, R. J., Middleton, B., Bell, G. D., & White, D. A. (1980). Inhibition of hepatic cholesterol synthesis and S-3-hydroxy-3-methylglutaryl-CoA reductase by mono and bicyclic monoterepenes administered. *In Vivo. Biochemical Pharmacology*, 29, 2125–2127. [https://doi.org/10.1016/0006-2952\(80\)90183-5](https://doi.org/10.1016/0006-2952(80)90183-5)
- Dash, S., Kumar, M., & Pareek, N. (2020). Enhanced antibacterial potential of berberine via synergism with chitosan nanoparticles. *Materials Today: Proceedings*, 31, 640–645. <https://doi.org/10.1016/j.matpr.2020.05.506>
- Devi, S. S., & Rajini, P. (2021). First report on post-harvest management of black mold of onion by eugenol. *South Asian Journal of Experimental Biology*, 11(6), 759–767. [https://doi.org/10.38150/sajeb.11\(6\).p](https://doi.org/10.38150/sajeb.11(6).p)
- Elsabee, M. Z., Morsi, R. E., & Al-Sabagh, A. M. (2009). Surface active properties of chitosan and its derivatives. *Colloids and Surfaces B: Biointerfaces*, 74, 1–16. <https://doi.org/10.1016/j.colsurfb.2009.06.021>
- Esmaeili, H., Cheraghi, N., Khanjari, A., Rezaeigolestani, M., Basti, A. A., Kamkar, A., et al. (2020). Incorporation of nanoencapsulated garlic essential oil into edible films: A novel approach for extending shelf life of vacuum-packed sausages. *Meat Science*, 166(108135). <https://doi.org/10.1016/j.meatsci.2020.108135>
- FDA (U.S. Food and Drug Administration). (2022). GHGA recalls various ready-to-eat vegetable products due to possible *Listeria monocytogenes* contamination. <https://www.fda.gov/safety/recalls-market-withdrawals-safety-alerts/ghga-recalls-various-ready-to-eat-vegetable-products-due-to-possible-listeria-monocytogenes-contaminant>
- Ferreira, A. R. V., Torres, C. A. V., Freitas, F., Sevrin, C., Grandfils, C., Reis, M. A. M., et al. (2016). Development and characterization of bilayer films of FucoPol and chitosan. *Carbohydrate Polymers*, 147, 8–15. <https://doi.org/10.1016/j.carbpol.2016.03.089>
- Finger, F. L., Santos, M. M., de S., Araujo, F. F., Lima, P. C. C., de Costa, et al. (2018). Action of essential oils on sprouting of non-dormant potato tubers. *Brazilian Archives of Biology and Technology*, 61, Article e18180003. <https://doi.org/10.1590/1678-4324-201818180003>
- Froio, F., Mosaddik, A., Morshed, M. T., Paolino, D., Fessi, H., & Elaissari, A. (2019). Edible polymers for essential oils encapsulation: Application in food preservation. *Industrial & Engineering Chemistry Research*, 58, 20932–20945. <https://doi.org/10.1021/acs.iecr.9b02418>
- Gennadios, A., Weller, C. L., Hanna, M. A., & Froning, G. W. (1996). Mechanical and barrier properties of egg albumen films. *Journal of Food Science*, 61(3), 585. <https://doi.org/10.1111/j.1365-2621.1996.tb13164.x>
- Gumbo, N., Magwaza, L. S., & Ngobese, N. Z. (2021). Evaluating ecologically acceptable sprout suppressants for enhancing dormancy and potato storability: A review. *Plants*, 10(11), 2307. <https://doi.org/10.3390/plants10112307>
- Gutiérrez, J., Barry-Ryan, C., & Bourke, P. (2008). The antimicrobial efficacy of plant essential oil combinations and interactions with food ingredients. *International Journal of Food Microbiology*, 124, 91–97. <https://doi.org/10.1016/j.ijfoodmicro.2008.02.028>
- Hambleton, A., Debeaufort, F., Bonnotte, A., & Voilley, A. (2009). Influence of alginate emulsion-based films structure on its barrier properties and on the protection of microencapsulated aroma compound. *Food Hydrocolloids*, 23, 2116–2124. <https://doi.org/10.1016/j.foodhyd.2009.04.001>
- Han, J. H., & Floros, J. D. (1997). Casting antimicrobial packaging films and measuring their physical properties and antimicrobial activity. *Journal of Plastic Film & Sheeting*, 13(4), 287–298. <https://doi.org/10.1177/875608799701300405>
- Hein, S., Wang, K., Stevens, W. F., & Kjems, J. (2008). Chitosan composites for biomedical applications: Status, challenges and perspectives. *Materials Science and Technology*, 24(9), 1053–1061. <https://doi.org/10.1179/174328408X341744>
- Hu, F., Tu, X. F., Thakur, K., Hu, F., Li, X. L., Zhang, Y. S., et al. (2019). Comparison of antifungal activity of essential oils from different plants against three fungi. *Food and Chemical Toxicology*, 134(110821). <https://doi.org/10.1016/j.fct.2019.110821>
- Hurst, W. C., Shewfelt, R. L., & Schuler, G. A. (1985). Shelf-life and quality changes in summer storage onions (*Allium cepa*). *Journal of Food Science*, 50(761). <https://doi.org/10.1111/j.1365-2621.1985.tb13791.x>
- Karaca, A. C., Nickerson, M., & Low, N. H. (2013). Microcapsule production employing chickpea or lentil protein isolates and maltodextrin: Physicochemical properties and oxidative protection of encapsulated flaxseed oil. *Food Chemistry*, 139, 448–457. <https://doi.org/10.1016/j.foodchem.2013.01.040>
- Kasaai, M. R. (2009). Various methods for determination of the degree of N-acetylation of chitin and chitosan: A review. *Journal of Agricultural and Food Chemistry*, 57, 1667–1676. <https://doi.org/10.1021/jf803001m>
- Khalil, A. A., Deraz, S. F., Elrahman, S. A., & El-Fawal, G. (2015). Enhancement of mechanical properties, microstructure, and antimicrobial activities of zein films cross-linked using succinic anhydride, eugenol, and citric acid. *Preparative Biochemistry & Biotechnology*, 45(6), 551–567. <https://doi.org/10.1080/10826068.2014.940967>
- Kleinkopf, G. E., Oberg, N. A., & Olsen, N. L. (2003). Sprout inhibition in storage: Current status, new chemistries and natural compounds. *American Journal of Potato Research*, 80, 317–327. <https://doi.org/10.1007/BF02854316>
- Marcuzzo, E., Sensidoni, A., Debeaufort, F., & Voilley, A. (2010). Encapsulation of aroma compounds in biopolymeric emulsion based edible films to control flavour release. *Carbohydrate Polymers*, 80, 984–988. <https://doi.org/10.1016/j.carbpol.2010.01.016>
- Marković, M., Momčilov, M. T., Uzelac, B., Radulović, O., Milošević, S., Jevremović, S., et al. (2020). Breaking the dormancy of snake's head fritillary (*Fritillaria meleagris* L.) in vitro bulbs – Part 2: Effect of GA₃ soaking and chilling on sugar status in sprouted bulbs. *Plants*, 9(1573). <https://doi.org/10.3390/plants9111573>
- Maw, B. W., Hung, Y. C., Tollner, E. W., Smittle, D. A., & Mullinix, B. G. (1996). Physical and mechanical properties of fresh and stored sweet onions. *Transactions of the ASAE*, 39(2), 633–637. <https://doi.org/10.13031/2013.27545>
- Miedema, P. (1994). Bulb dormancy in onion. I. The effects of temperature and cultivar on sprouting and rooting. *Journal of Horticultural Science*, 69(1), 29–39. <https://doi.org/10.1080/14620316.1994.11515245>
- Morcia, C., Malnati, M., & Terzi, V. (2012). *In vitro* antifungal activity of terpinen-4-ol, eugenol, carvone, 1,8-cineole (eucalyptol) and thymol against mycotoxigenic plant pathogens. *Food Additives & Contaminants: Part A*, 29(3), 415–422. <https://doi.org/10.1080/19440049.2011.643458>
- Moser, P., Ferreira, S., & Nicoletti, V. R. (2019). Buriti oil microencapsulation in chickpea protein-pectin matrix as affected by spray drying parameters. *Food and Bioprocess Technology*, 117, 183–193. <https://doi.org/10.1016/j.fbp.2019.07.009>
- NBPSDHU (North Bay Parry Sound District Health Unit). (2009). *Investigative summary of the Escherichia coli outbreak associated with a restaurant in North Bay, Ontario: October to November 2008*.
- Nisar, T., Wang, Z. C., Yang, X., Tian, Y., Iqbal, M., & Guo, Y. (2018). Characterization of citrus pectin films integrated with clove bud essential oil: Physical, thermal, barrier, antioxidant and antibacterial properties. *International Journal of Biological Macromolecules*, 106, 670–680. <https://doi.org/10.1016/j.ijbiomac.2017.08.068>
- Oosterhaven, K., Hartmans, K. J., & Huizing, H. J. (1993). Inhibition of potato (*Solanum tuberosum*) sprout growth by the monoterpene S-carvone: Reduction of 3-hydroxy-3-methylglutaryl coenzyme a reductase activity without effect on its mRNA level. *Journal of Plant Physiology*, 141(4), 463–469. [https://doi.org/10.1016/S0176-1617\(11\)80195-1](https://doi.org/10.1016/S0176-1617(11)80195-1)
- Oussalah, M., Caillet, S., Saucier, L., & Lacroix, M. (2007). Inhibitory effects of selected plant essential oils on the growth of four pathogenic bacteria: *E. coli* O157:H7, *Salmonella* Typhimurium, *Staphylococcus aureus* and *Listeria monocytogenes*. *Food Control*, 18, 414–420. <https://doi.org/10.1016/j.foodcont.2005.11.009>
- Perumal, A. B., Huang, L., Nambiar, R. B., He, Y., Li, X., & Sellamuthu, P. S. (2022). Application of essential oils in packaging films for the preservation of fruits and vegetables: A review. *Food Chemistry*, 375(131810). <https://doi.org/10.1016/j.foodchem.2021.131810>
- Rokita, B., Czechowska-Biskup, R., & Ulanski, P. (2005). Modification of polymers by ultrasound treatment in aqueous solution. *E-Polymers*, 5(1), 24. <https://doi.org/10.1515/epoly.2005.5.1.261>
- Roldán-Marín, E., Sánchez-Moreno, C., de Ancos, R. L. B., & Cano, P. (2009). Onion high-pressure processing: Flavonol content and antioxidant activity. *LWT - Food Science and Technology*, 42, 835–841. <https://doi.org/10.1016/j.lwt.2008.11.013>
- Sabphon, C., Srichoosilp, A., Wanichwecharungruang, S., Sukwattanasinitt, M., Vadhanasindhu, P., Ngamchuachit, P., et al. (2020). Dissolvable and edible film for long-lasting kaffir lime aroma in food. *International Journal of Food Science and Technology*, 55, 1523–1530. <https://doi.org/10.1111/ijfs.14426>
- Santin, J. R., Lemos, M., Klein-Júnior, Machado, I. D., Costa, P., de Oliveira, A. P., et al. (2011). Gastroprotective activity of essential oil of the *Syzygium aromaticum* and its major component eugenol in different animal models. *Naunyn-Schmiedeberg's Archives of Pharmacology*, 383, 149–158. <https://doi.org/10.1007/s00210-010-0582-x>
- Santos, A. L., Chierice, G. O., Alexander, K. S., Riga, A., & Matthews, E. (2009). Characterization of the raw essential oil eugenol extracted from *Syzygium aromaticum* L. *Journal of Thermal Analysis and Calorimetry*, 96(3), 821–825. <https://doi.org/10.1007/s10973-009-0030-7>
- Santos, M. N., de S., Araujo, F. F., de Lima, P. C. C., da Costa, et al. (2020). Changes in potato tuber sugar metabolism in response to natural sprout suppressive compounds. *Acta Scientiarum. Agronomy*, 42, Article e43234. <https://doi.org/10.4025/actasciagron.v42i1.43234>
- Schulz, P. C., Rodríguez, M. S., Del Blanco, L. F., Pistonesi, M., & Agulló, E. (1998). Emulsification properties of chitosan. *Colloid and Polymer Science*, 276, 1159–1165. <https://doi.org/10.1007/s003960050359>
- Shakoor, I. F., Pamunuwa, G. K., & Karunaratne, D. N. (2023a). Efficacy of alginate and chickpea protein polymeric matrices in encapsulating curcumin for improved stability, sustained release and bioaccessibility. *Food Hydrocolloids for Health*, 3(100119). <https://doi.org/10.1016/j.fhfh.2023.100119>
- Shakoor, I. F., Pamunuwa, G. K., & Karunaratne, D. N. (2023b). Chickpea and soybean protein delivery systems for oral ingestion of hydroxycitric acid. *Food Chemistry Advances*, 2(100207). <https://doi.org/10.1016/j.focha.2023.100207>
- Sharma, S., Mulrey, L., Byrne, M., Jaiswal, A. K., & Jaiswal, S. (2022). Encapsulation of essential oils in nanocarriers for active food packaging. *Foods*, 11(2337). <https://doi.org/10.3390/foods11152337>
- Sheikh, F. R., Jose-Santhi, J., Kalia, D., Singh, K., & Singh, R. K. (2022). Sugars as the regulators of dormancy and sprouting in geophytes. *Industrial Crops & Products*, 189(115817). <https://doi.org/10.1016/j.indcrop.2022.115817>
- Shen, C., Chen, W., Li, C., Aziz, T., Cui, H., & Lin, L. (2023). Topical advances of edible coating based on the nanoemulsions encapsulated with plant essential oils for foodborne pathogen control. *Food Control*, 145(109419). <https://doi.org/10.1016/j.foodcont.2022.109419>

- Singleton, V. L., & Rossi, J. A. (1965). Colorimetry of total phenolics with phosphomolybdic-phosphotungstic acid agents. *American Journal of Enology and Viticulture*, 16(3), 144–158. <https://doi.org/10.5344/ajev.1965.16.3.144>
- Suttle, J. C., Olson, L. L., & Lulai, E. C. (2016). The involvement of gibberellins in 1,8-cineole-mediated inhibition of sprout growth in russet burbank tubers. *American Journal of Potato Research*, 93, 72–79. <https://doi.org/10.1007/s12230-015-9490-4>
- Temkin-Gorodeiski, N., Kahan, R. S., & Padova, R. (1972). Development of damage in the buds during storage of irradiated onions. *Canadian Journal of Plant Science*, 52(5), 817–826. <https://doi.org/10.4141/cjps72-133>
- Upadhyay, A., Upadhyaya, I., Karumathil, D. P., Yin, H. B., Nair, M. S., Bhattaram, V., et al. (2015). Control of *Listeria monocytogenes* on skinless frankfurters by coating with phytochemicals. *LWT - Food Science and Technology*, 63, 37–42. <https://doi.org/10.1016/j.lwt.2015.03.100>
- Verlee, A., Mincke, S., & Stevens, C. V. (2017). Recent developments in antibacterial and antifungal chitosan and its derivatives. *Carbohydrate Polymers*, 164, 268–283. <https://doi.org/10.1016/j.carbpol.2017.02.001>
- Wang, H., Qian, J., & Ding, F. (2018). Emerging chitosan-based films for food packaging applications. *Journal of Agricultural and Food Chemistry*, 66, 395–413. <https://doi.org/10.1021/acs.jafc.7b04528>
- Xie, Y., Huang, Q., Wang, Z., Cao, H., & Zhang, D. (2017). Structure-activity relationships of cinnamaldehyde and eugenol derivatives against plant pathogenic fungi. *Industrial Crops and Products*, 97, 388–394. <https://doi.org/10.1016/j.indcrop.2016.12.043>
- Xue, F., Gu, Y., Li, C., & Adhikari, B. (2019). Encapsulation of essential oil in emulsion based edible films prepared by soy protein isolate-gum acacia conjugates. *Food Hydrocolloids*, 96, 178–189. <https://doi.org/10.1016/j.foodhyd.2019.05.014>
- Yemencioğlu, A. (2022). *Edible food packaging with natural hydrocolloids and active agents* (1st ed.). Boca Raton, USA: CRC Press.
- Zhang, W., Jiang, H., Rhim, J. W., Cao, J., & Jiang, W. (2022). Effective strategies of sustained release and retention enhancement of essential oils in active food packaging films/coatings. *Food Chemistry*, 367(130671). <https://doi.org/10.1016/j.foodchem.2021.130671>
- Zhang, H., Liang, Y., Li, X., & Kang, H. (2020). Effect of chitosan-gelatin coating containing nano-encapsulated tarragon essential oil on the preservation pork slices. *Meat Science*, 166(108137). <https://doi.org/10.1016/j.meatsci.2020.108137>
- Zhang, J., Tian, Y., Wang, J., Ma, J., Liu, L., Islam, R., et al. (2023). Inhibitory effect and possible mechanism of oregano and clove essential oils against *Pectobacterium carotovorum* subsp. *carotovorum* as onion soft rot in storage. *Postharvest Biology and Technology*, 196(112164). <https://doi.org/10.1016/j.postharvbio.2022.112164>
- Zhang, Y., Wang, Y., Zhu, X., Cao, P., Wei, S., & Lu, Y. (2017). Antibacterial and antibiofilm activities of eugenol from essential oil of *Syzygium aromaticum* (L.) Merr. & L. M. Perry (clove) leaf against periodontal pathogen *Porphyromonas gingivalis*. *Microbial Pathogenesis*, 113, 396–402. <https://doi.org/10.1016/j.micpath.2017.10.054>
- Zhang, P., Zhao, Y., & Shi, Q. (2016). Characterization of a novel edible film based on gum ghatti: Effect of plasticizer type and concentration. *Carbohydrate Polymers*, 153, 345–355. <https://doi.org/10.1016/j.carbpol.2016.07.082>
- Ziani, K., Fang, Y., & McClements, D. J. (2012). Encapsulation of functional lipophilic components in surfactant-based colloidal delivery systems: Vitamin E, vitamin D, and lemon oil. *Food Chemistry*, 134, 1106–1112. <https://doi.org/10.1016/j.foodchem.2012.03.027>
- Zidan, A. S., Sammour, O. A., Hammad, M. A., Megrab, N. A., Habib, M. J., & Khan, M. A. (2007). Quality by design: Understanding the product variability of a self-nanoemulsified drug delivery system of cyclosporine A. *Journal of Pharmaceutical Sciences*, 96(9), 2409–2423. <https://doi.org/10.1002/jps.20824>